Limnol. Oceanogr., 57(6), 2012, 1757–1774

doi:10.4319/lo.2012.57.6.1757

Elemental and isotopic characterization of dissolved and particulate organic matter in a unique California upwelling system: Importance of size and composition in the export of labile material

B. D. Walker[1,*] and M. D. McCarthy

Department of Ocean Science, University of California, Santa Cruz, California

Abstract

We report the interseasonal variation in bulk elemental and stable isotopic ($\delta^{13}C$, $\delta^{15}N$) composition of dissolved and particulate organic matter (DOM, POM) during a high-resolution time series (2007–2009) on the Big Sur coast. In addition to interseasonal variations, we explore the relationships between physical size and reactivity (i.e., composition) of exportable organic matter (OM) pools, and characterize the elemental and isotopic composition of size-fractionated POM and DOM pools within this potentially high-nutrient, low-chlorophyll (HNLC) California upwelling region. Average POM concentrations were low (< 5.2 μmol C L^{-1} and $<$ 0.7 μmol N L^{-1}), and all OM pools had low C : N ratios (DOM average = 15.0 and POM < 7.8)—indicating that this upwelling center may represent an important source of N-rich material to offshore environments. Seasonal "excess" dissolved organic carbon (DOC) production was significant ($\sim$ 30–80 μmol L^{-1} DOC); however, dissolved organic nitrogen (DON) production and cycling was largely decoupled from both DOC and physical processes. Overall, our results are consistent with this region representing an "HNLC upwelling system." The distinct bulk elemental and isotopic OM composition and seasonality vs. that of high-productivity upwelling regions highlights the need to better understand the biogeochemical diversity of upwelling systems. Finally, we observed a quantifiable size–composition relationship across both POM and DOM size classes, perhaps representing a powerful new tool for modeling N vs. C fluxes in ocean biogeochemical cycles.

Coastal upwelling regions are among the most dynamic and important components of the modern ocean carbon cycle. While they make up only about 1% of ocean surface area, they are responsible for over 10% of global new production in terms of global carbon sequestration (Chavez and Toggweiler 1995). Recent work suggests that these regions are even more important than previously recognized and could be responsible for $> 40\%$ of all ocean carbon burial in the modern ocean (Muller-Karger et al. 2005). The central California coast is located at the center of a major global upwelling region, within the California Current System (CCS). Both measurements and models suggest that sea-to-air degassing of upwelled CO_2 is greatly attenuated by biological activity, and that the majority of this fixed carbon is exported as dissolved and suspended particulate organic matter (DOM, POM; Barth et al. 2002; Hales et al. 2005; N. Gruber unpubl.). Recent studies have shown that a major fraction of margin-derived organic matter (OM) appears to be seasonally exported offshore—representing a major source of labile OM to open ocean and mesopelagic environments (Alvarez-Salgado et al. 2001*a*; Hill and Wheeler 2002; Wetz and Wheeler 2003). For example, extracellular release of DOM by phytoplankton has been noted as an important mechanism for DOM production within equatorial and coastal upwelling systems (Bronk 2002; Wetz and Wheeler 2007). However, only a few studies have examined POM and DOM composition in the context of production and export from upwelling systems (e.g., coastal Oregon and the NW Iberian Peninsula; Alvarez-Salgado et al. 2001*a*; Hill and Wheeler 2002).

Recent work has also suggested that a large portion of the central California coast, spanning $\sim$ 300 km along the Big Sur coastline, may be iron limited. Here, a very narrow continental shelf is hypothesized to result in a lack of micronutrients (e.g., iron) and lower primary productivity (Hutchins and Bruland 1998; Bruland et al. 2001). If correct, this coastal upwelling system may represent an iron-deplete, high-nutrient, low-chlorophyll (HNLC) region. It is also possible that water column detrital OM pools are geochemically distinct from those in more "classical" high-productivity coastal upwelling systems (e.g., the Oregon coast or Monterey Bay). The biogeochemistry of detrital OM pools produced, recycled, and exported from an HNLC upwelling region has never been directly investigated. If important differences exist between OM pools in distinct upwelling regions of the CCS, this might have significant implications for biogeochemical models of margin carbon and nitrogen export.

Previous work has shown that the relative molecular size of detrital (nonliving) OM can be linked to its microbial reactivity and degradation rate in the ocean. Larger size fractions of DOM and POM generally have "fresher" chemical compositions, are more bioavailable, and have faster turnover rates (Amon and Benner 1994; Benner et al. 1997; Sannigrahi et al. 2005). In a coastal upwelling system, OM size might also be closely related to its transport and fate. For POM, large particles with fast sinking rates would

* Corresponding author: brett.walker@uci.edu

[1] Present address: Department of Earth System Science, Keck Carbon Cycle Accelerator Mass Spectrometry Laboratory, University of California, Irvine, California

contribute to increased local burial, while small suspended particles can be advected great distances—potentially exporting coastal material far from continental margins (Bauer and Druffel 1998). In the case of DOM, the high-molecular-weight (HMW) DOM size fraction is generally "chemically fresh," has younger ^{14}C ages, and is more bioavailable than total DOM (Amon and Benner 1994; Repeta and Aluwihare 2006; Walker et al. 2011). Therefore, the isolation of HMW DOM allows for the direct examination of labile DOM composition and export to offshore and/or mesopelagic ecosystems. While a relationship between OM size and composition has never been explicitly examined within a coastal upwelling system, this could have considerable implications for estimating the fate of OM exported from coastal upwelling regions.

Here we present a biweekly, 1.5 yr geochemical time series of POM and DOM collected from September 2007 to April 2009 on the Big Sur coast. Main goals of this study are to: (1) assess the interseasonal variability in abundance and bulk composition of POM and DOM produced within this potential HNLC upwelling center and (2) examine the linkages between this variability to both physical and biological processes. We measured the concentration, elemental composition (i.e., molar C : N ratio), and both $\delta^{13}C$ and $\delta^{15}N$ stable isotopic composition of detrital OM pools throughout major CCS oceanographic periods. We also isolated size-fractionated POM and DOM samples (via micro- and ultrafiltration) during these CCS oceanographic periods, allowing us to assess changes in OM size classes. This study provides a comprehensive evaluation of detrital OM pools in a unique, relatively unstudied upwelling center and also provides the first direct examination of coastal OM size vs. composition relationships between all major OM pools.

Methods

Study site—The time series was conducted at the Granite Canyon Marine Pollution Studies Laboratory (GCMPSL)—an active Scripps Institute of Oceanography (SIO) Shore Stations monitoring site since 1971. The GCMPSL is located along the Big Sur coast and Santa Lucia range, far from known pollution sources, on a narrow continental shelf just south of Carmel, California (Fig. 1; 36°26′24″N, 121°55′19″W). At the GCMPSL, a seawater intake system delivers seawater from a nearshore channel (3 m depth) to a ~ 120,000 liter hypalon-lined tank (elevation 40 m). The tank is continuously flushed, and seawater residence times were less than 4 h. An intake pipe 0.5 m off the tank bottom continuously supplies this seawater by gravity. Despite the fact that this is a shore-based station, due to the narrow shelf and specific location within southward flow of the CCS, seawater at GCMPSL has been previously shown to be highly representative of CCS waters (Shkedy et al. 1995; Breaker 2005). The detailed analysis we provide below (Results and Discussion) for OM composition, physical and hydrographic data, and a tank vs. channel comparison (Table 1) also strongly support this interpretation.

Hydrographic sample collection and analysis—Sea surface temperature (SST) and salinity data were collected as part of the SIO Shore Stations program (http://shorestation.ucsd.edu/). SST was determined at 1 m depth using a mercury immersion thermometer (Kahl Scientific Instruments; 0.01°C accuracy). Seawater salinity is reported in Practical Salinity Scale (PSS) to 0.01 (UNESCO 1981). Wind velocity (m s^{-1}) and compass heading data were obtained from the GCMPSL meteorological station courtesy of D. Lind at the Marine Atmospheric Measurements Laboratory, Naval Postgraduate School. Daily average Upwelling index (UI; m^3 s^{-1} 100 m^{-1} coastline) data were obtained from National Oceanographic and Atmospheric Association (NOAA) Pacific Fisheries Environmental Laboratory (PFEL; http://www.pfeg.noaa.gov/) for National Buoy Data Center (NBDC) Sta. No. 46042 (36°47′19″N, 122°24′15″W).

Dissolved sample collection and analysis—All biweekly dissolved seawater samples were collected from filtrates of precombusted (450°C, 4 h) ~ 0.7 μm glass-fiber filters (GF/F; Whatman 25 mm). All glassware used for dissolved sample collection and storage was first cleaned using detergent (FL-70), 10% HCl, and 18.2 MΩ Milli-Q water, and combusted at 450°C for 4 h. Nutrient samples—nitrate plus nitrite (hereafter referred to as nitrate), phosphate, silicic acid, and ammonium—were collected into 250 mL acid-cleaned (10% HCl) dark high-density polyethylene (HDPE) bottles, transported on ice, and stored in the dark at −20°C until analysis on a Lachat Quikchem 8000 Flow Injection Analyzer (Smith and Bogren 2001*a,b*; Knepel and Bogren 2002). Replicate nutrient sample standard deviations were less than ± 0.2 μmol L^{-1} for nitrate and silicate and less than ± 0.04 μmol L^{-1} for phosphate and ammonium.

Dissolved organic carbon (DOC) and total dissolved nitrogen (TDN) samples were collected using a 2 liter glass filter manifold. This volume was then decanted into precombusted 24 mL borosilicate vials, transported on ice, and stored in the dark at −20°C until sample analysis. DOC and dissolved organic nitrogen (DON) samples were analyzed via high temperature combustion using a Shimadzu total organic carbon and nitrogen analyzer (model TOC-V/TNM-1) and corrected to consensus reference material values (Hansell 2005; Carlson et al. 2010). Errors represent the standard deviation of $n = 3$ sample replicates per sample date. Reported DON concentrations were determined after subtracting independently measured nitrate + nitrite and ammonium values from TDN data and propagating errors (Bronk et al. 2000).

The presence of high dissolved inorganic nitrogen (DIN) can result in higher relative standard deviations (i.e., high coefficients of variation; %CV) of DON (Bronk et al. 2000; Sharp et al. 2002). In addition, low DON can result in an exponential increase in DOM C : N ratios as DON approximates zero. With this in mind, we used two simple constraints in reporting our averaged seasonal estimates of DON concentrations and DOM C : N ratios (shown in Table 2). First, we included only data where DON %CV ≤ 30, prior to exponential increases in %CV resulting from a decreasing DON : DIN ratio. Second, DON concentrations ≤ 1.0 μmol N L^{-1} were excluded to avoid anomalously

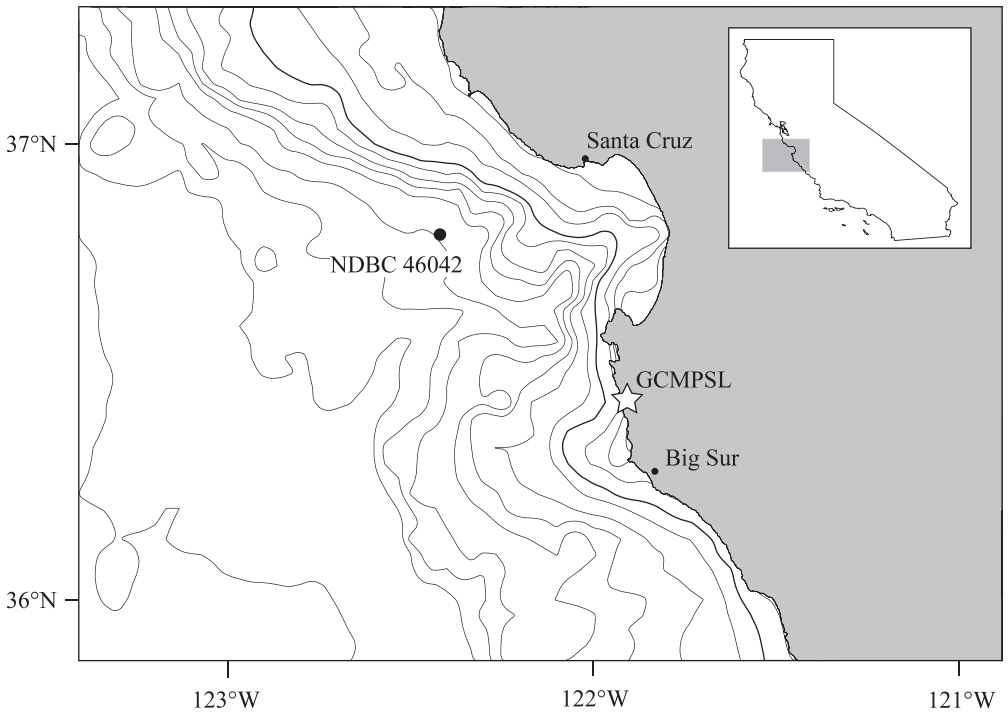

Fig. 1. The location of the Granite Canyon Marine Pollutions Studies Laboratory (GCMPSL). The GCMPSL is indicated by a star in relation to Monterey Bay and the Central Coast of California. Inlayed map shows the relative location of the Monterey Bay area with respect to the California coastline. Bathymetric contours represent the following depths (m): 50, 100, 200, 500 (bold), 700, 1000, 1250, 1500, 2000, 2500, 3000, and 3500.

high DOM C : N ratios. These constraints resulted in the exclusion of only six DON measurements from our total sample set ($n = 41$). However, they reduced any potential bias that a few individual high DOM C : N ratios (> 70) would have on averaged CCS DOM C : N ratios (i.e., where DOC remained high, but very low DON concentrations coupled with high %CV and propagated errors made DON values unreliable).

Suspended POM—Biweekly suspended POM samples were collected by gravity feed of 12–16 liters of seawater onto precombusted (450°C, 4 h) 25 mm diameter, 0.7 μm borosilicate GF/F filters using acid-cleaned 10 liter HDPE carboys, silicone tubing, and polycarbonate filter manifolds (hereafter referred to as GF/F-POM). Sample water was prefiltered using mesh netting (500 μm) to remove large detritus and mesozooplankton. After collection, GF/F filters were placed on precombusted aluminum foil, transported on ice, and stored in the dark at −20°C until sample processing. Particulate organic carbon and nitrogen (POC, PON) concentrations were determined by high temperature combustion elemental (CHN) and isotopic analysis, using known seawater volumes.

Large-volume POM and HMW DOM sample collection—Large-volume (1600 to 4000 liters) ultrafiltered POM (UPOM) samples were isolated from prefiltered seawater (< 100 μm) using high-shear conditions previously described by Roland et al. (2009), using a 0.1 μm hollow-fiber membrane (Amersham Biosciences, model CFP-1-E-55). Sample water was prefiltered using 100 μm mesh filter bags in an acid-cleaned polycarbonate housing (McMaster-Carr). UPOM samples were reduced to ~ 10 liters, diafiltered in the field using 10 liters of 18.2 MΩ Milli-Q water, reduced to ~ 1 liter, and collected into acid-cleaned polycarbonate bottles. UPOM samples were first frozen and stored in the dark at −20°C and later dried via centrifugal evaporation prior to CHN analysis. Overall UPOM recoveries ($n = 10$) averaged 36.5% ± 16% C and 35.3% ± 16.2% N of GF/F-POM. These values are consistent with previously reported surface-water recoveries using ~ 0.1 μm hollow-fiber membranes in the Pacific Ocean (~ 48% ± 8%, $n = 7$ by Benner et al. 1997; ~ 22%, $n = 1$ by Roland et al. 2009), and represented 10–57% of GF/F-POC.

HMW DOM samples (1 nm–0.1 μm) were collected following the methods described previously in Walker et al. (2011) using GE Osmonics membranes (nominal molecular weight cut-off = 2.5 kDa, model GE2540-F1072). Briefly, seawater supplying the ultrafiltration system was prefiltered using double open end (DOE) filters (100 μm and 20 μm) in stainless steel housings placed upstream of an acid-cleaned (10% HCl) 0.1 μm polyethersulfone cartridge filter (Pall). Seawater volumes of ~ 1500–2000 liters were concentrated to 2 liters in the field and stored at −20°C; later they were diafiltered with 20 liters of 18.2 MΩ Milli-Q water and dried via centrifugal evaporation prior to CHN analyses. Our HMW DOM isolations retained between 9% and 23% of

Table 1. Summary of GCMPSL physical and hydrographic data. Sample dates followed by T and C represent contemporaneous samples taken from the GCMPSL seawater intake system tank (T) and the channel (C) adjacent to the lab. ND, data not determined.

Sample date	SST (°C)	Salinity	σ_t (kg m^{-3})	Spiciness π	UI (3 day average; m^3 s^{-1} 100 m^{-1} coast)	Nitrate (μmol L^{-1})	Silicic acid (μmol L^{-1})	Ammonium (μmol L^{-1})	Phosphate (μmol L^{-1})
21 Sep 07	11.7	33.89	25.78	0.57	36	8.3	7.5	2.16	0.28
22 Sep 07	ND	ND	ND	ND	2	16.1	14.0	ND	0.73
23 Sep 07	ND	ND	ND	ND	11	13.3	10.0	5.26	0.65
24 Sep 07	ND	ND	ND	ND	20	10.3	8.9	3.77	0.47
25 Sep 07	14.5	33.73	25.10	1.01	27	9.8	8.5	2.65	0.39
09 Oct 07	12.3	33.83	25.62	0.64	17	21.1	17.6	2.72	1.45
12 Nov 07	ND	ND	ND	ND	54	14.6	12.4	1.64	0.70
27 Nov 07	12.4	33.59	25.42	0.47	62	14.0	12.0	2.42	0.74
14 Dec 07	11.5	33.59	25.59	0.29	42	15.1	12.9	1.66	0.76
16 Jan 08	11.5	33.63	25.62	0.32	72	7.4	5.9	1.73	0.24
29 Jan 08	11.8	33.35	25.35	0.16	0	5.7	6.1	3.16	0.24
12 Feb 08	12.1	33.60	25.48	0.41	73	6.7	5.4	4.59	0.15
29 Feb 08	11.9	33.52	25.46	0.31	78	10.8	9.9	0.81	0.85
01 Mar 08	11.5	33.64	25.63	0.33	125	13.9	12.6	0.83	1.04
02 Mar 08	10.1	33.76	25.97	0.18	134	23.8	24.3	0.59	1.08
18 Mar 08	9.8	34.12	26.30	0.41	167	27.2	32.3	8.13	1.21
01 Apr 08	10.2	34.11	26.22	0.47	72	11.0	11.3	1.39	0.48
14 Apr 08	10.3	34.19	26.27	0.55	147	18.2	18.8	ND	0.79
28 Apr 08	10.0	34.15	26.29	0.47	143	25.8	30.7	0.82	1.09
09 May 08	9.8	34.05	26.24	0.35	155	16.2	17.8	0.57	0.64
10 May 08	10.0	34.09	26.24	0.42	116	14.5	16.0	0.67	0.50
11 May 08	9.9	34.07	26.24	0.39	125	31.5	34.9	0.70	1.40
28 May 08	11.3	33.89	25.86	0.49	22	11.6	13.7	0.93	0.41
12 Jun 08	10.3	34.24	26.31	0.59	100	14.1	15.9	0.75	0.45
27 Jun 08	12.1	33.77	25.62	0.55	91	17.7	18.1	1.81	0.67
09 Jul 08	12.7	33.82	25.54	0.71	21	21.0	21.9	1.04	0.92
23 Jul 08	12.1	33.92	25.73	0.67	82	25.8	24.8	0.70	0.97
06 Aug 08	11.9	33.86	25.72	0.58	52	15.1	17.5	ND	0.60
21 Aug 08	13.7	33.69	25.24	0.81	65	6.9	8.9	1.51	0.32
12 Sep 08	14.9	33.60	24.92	1.00	33	4.9	11.4	2.61	0.38
13 Sep 08	14.8	33.58	24.92	0.96	31	6.0	7.8	2.61	0.46
14 Sep 08	14.5	33.59	24.99	0.90	24	3.2	4.8	2.83	0.16
15 Sep 08	14.7	33.63	24.98	0.98	21	10.4	11.1	2.29	0.67
23 Sep 08	12.3	33.59	25.44	0.45	54	5.2	5.8	1.86	0.22
24 Sep 08	12.6	33.59	25.38	0.50	31	12.9	12.6	1.46	0.68
18 Oct 08	12.8	33.47	25.25	0.45	24	13.5	11.6	1.83	0.99
26 Nov 08	13.1	33.40	25.13	0.46	−13	8.7	7.5	1.13	0.69
17 Dec 08	12.0	33.49	25.42	0.31	32	12.4	9.9	2.29	0.87
15 Jan 09T	12.5	33.62	25.42	0.51	12	10.8	9.7	1.73	0.96
15 Jan 09C	12.5	33.62	25.42	0.51	12	10.2	9.3	1.97	0.94
05 Feb 09	12.9	33.44	25.20	0.45	−22	5.0	5.9	1.37	0.44
10 Feb 09	12.2	33.50	25.39	0.35	88	7.0	7.6	1.34	0.71
26 Feb 09	12.5	33.25	25.14	0.22	45	8.5	9.0	1.13	0.77
10 Mar 09	10.3	33.80	25.96	0.24	106	19.8	19.8	1.19	1.42

total DOC, consistent with previously published HMW DOM recoveries (Benner et al. 1997; Loh et al. 2004; Walker et al. 2011). HMW DOC concentrations follow an identical trend to that of total DOC ($R^2 = 0.80$, $p = 0.0004$), strongly indicating that the HMW DOC isolated in this study accurately reflects the abundance and variability of HMW DOC at the GCMPSL.

Stable isotopic analysis—Stable carbon ($\delta^{13}C$) and nitrogen ($\delta^{15}N$) isotopic analysis was performed at the University of California, Santa Cruz, Stable Isotope Laboratory by CHN analysis using a Carlo Erba CHNO-S EA-1108 Elemental Analyzer and Thermo-Finnigan Delta Plus XP isotope ratio mass spectrometer. Elemental ratios reported herein represent the ratio of molar carbon and nitrogen concentrations (C : N ratios). For POM samples, GF/F filters were vapor-acidified (12 mol L^{-1} HCl, 12 h) and oven-dried overnight (50°C) prior to CHN analysis. UPOM and HMW DOM samples were directly acidified with 1 mol L^{-1} HCl in either silver capsules or precombusted (450°C, 4 h) quartz tubes and oven-dried overnight prior to CHN analysis. Results are reported in standard per mil (‰) notation and relative to Vienna Pee Dee Belemnite (V-PDB) for $\delta^{13}C$ and to air for $\delta^{15}N$.

Table 2. Average bulk chemical composition of total and size-fractionated high-molecular-weight (HMW) DOM and POM (GF/F-POM and "ultrafiltered" UPOM) pools are reported for the three main oceanographic seasons affecting the GCMPSL (Oceanic, Davidson, Upwelling). Bold values represent the mean of all samples collected within the specified date ranges. SD represents the 1 σ standard deviations of the sample population (n) only when $n \geq 3$ samples were measured. For $n = 2$, SD represents the range in values; for $n = 1$, SD is not reported. ND, data not determined.

	Oceanic	Davidson	Upwelling	Oceanic	Davidson
Detrital OM pool	21 Sept 07–12 Nov 07	27 Nov 07–02 Mar 08	18 Mar 08–09 Jul 08	23 Jul 08–18 Oct 08	26 Nov 08–10 Mar 09
GF/F-POC (μmol L^{-1})					
mean	4.23	3.29	3.44	4.85	5.2
SD (n)	0.91(7)	0.6(8)	0.81(11)	0.9(9)	2.26(8)
GF/F-PON (μmol L^{-1})					
mean	0.61	0.48	0.52	0.73	0.7
SD (n)	0.13(7)	0.1(8)	0.14(11)	0.13(9)	0.26(8)
GF/F-POM C : N*					
mean	6.9	6.9	6.6	6.6	7.4
SD (n)	0.37(7)	0.46(8)	0.29(11)	0.28(10)	1.12(8)
GF/F-POM δ^{13}C (‰)					
mean	−21.64	−23.10	−21.58	−19.14	−21.76
SD (n)	0.72	1.41	0.83	0.91	0.92
GF/F-POM δ^{15}N (‰)					
mean	5.43	5.81	5.74	7.01	6.51
SD (n)	0.45	2.00	0.59	1.51	1.49
UPOC (μmol L^{-1})					
mean	1.75	0.87	0.22	2.68	ND
SD (n)	0.32(4)	0.55(2)	—(1)	1.08(3)	
UPON (μmol L^{-1})					
mean	0.24	0.12	0.03	0.40	ND
SD (n)	0.04(4)	0.07(2)	—(1)	0.16(3)	
UPOM C : N*					
mean	7.34	7.23	7.80	6.68	ND
SD (n)	0.29(4)	0.56(2)	—(1)	0.07(3)	
UPOM δ^{13}C (‰)					
mean	−21.03	−21.22	−22.02	−18.14	ND
SD	0.95	1.88	—(1)	0.93	
UPOM δ^{15}N (‰)					
mean	4.30	3.31	5.20	5.87	ND
SD	0.65	0.24	—(1)	0.60	
DOC (μmol L^{-1})					
mean	85.9	79.8	53.9	132.9	118.1
SD (n)	9.1(6)	15.4(8)	8.2(10)	47(10)	15.6(8)
DON (μmol L^{-1})					
mean	6.1	6.9	8.4	8.3	6.7
SD (n)	5.9(6)	4.1(8)	7.4(10)	4.2(10)	1.0(8)
DOM C : N*					
mean	13.9	15.5	7.9	18.3	17.8
SD (n)	10.5(4)	8.6(8)	8.5(7)	15.6(9)	2.1(8)
HMW DOM C : N†					
mean	11.4	9.9	10.2	11.9	ND
SD (n)	1.1(4)	0.1(2)	0.7(2)	0.9(3)	
HMW DOM δ^{13}C (‰)					
mean	−20.78	−19.31	−20.54	−18.44	ND
SD	0.48	0.66	0.66	0.79	
HMW DOM δ^{15}N (‰)					
mean	5.77	5.08	6.19	7.06	ND
SD	1.53	0.23	0.23	0.17	

* Total DOM C : N ratios with DON $\leq$ 1.0 μmol L^{-1} were excluded.
† C : N molar ratios values determined by CHN analysis.

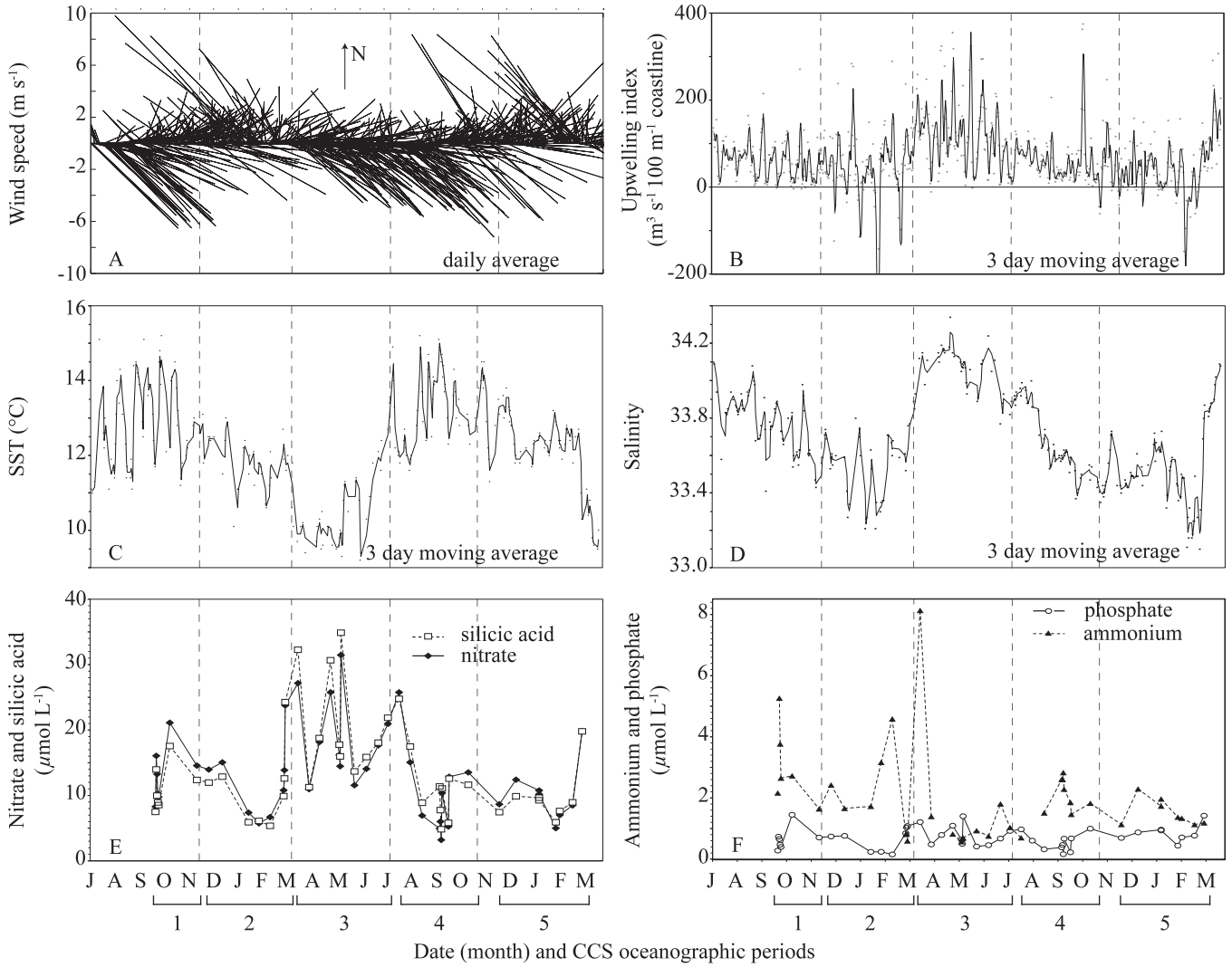

Fig. 2. Wind and hydrographic data are shown for the GCMPSL time series. (A–F) sample dates are shown by month from July 2007–April 2009. Vertical dashed lines denote CCS oceanographic periods. Here numbers 1 to 5 correspond to CCS oceanographic periods as described in the Results: Oceanic 2007, Davidson 2007, Upwelling 2008, Oceanic 2008, and Davidson 2008 periods, respectively.

Average external precision based on $n = 3$ sample replicates was ± 0.3‰ and ± 0.5‰ for $\delta^{13}C$ and $\delta^{15}N$, respectively.

Results

Hydrographic data and assessment—The hydrography at the GCMPSL is strongly influenced by seasonal changes in overlying wind stress, consistent with previous observations and correlations of wind stress to water mass properties ($r > 0.65$; Shkedy et al. 1995; Breaker 2005). Persistent northerly winds (≥ 4 m s^{-1}) were observed during spring and summer months, with infrequent onshore or wind relaxation events (Fig. 2A). Relaxed wind conditions were present in the winter months, punctuated by a few storm events creating strong southerly winds (4–10 m s^{-1}). An average daily UI (Fig. 2B; Table 1) shows upwelling-favorable conditions were present throughout most of the year, with the strongest upwelling conditions (UI = 100–300 m^3 s^{-1} 100 m^{-1} coastline) observed during spring/summer months. Only a few downwelling events occurred during winter months (UI = −50 to −100 m^3 s^{-1} 100 m^{-1} coastline) when low-pressure systems and winter storms influence the central California coast. One very pronounced storm event in late January produced extremely strong downwelling conditions (−460 m^3 s^{-1} 100 m^{-1} coastline).

Salinity and SST were negatively correlated ($R^2 = 0.37$, $p < 0.0001$) and displayed large seasonal offsets (Fig. 2C,D). SST ranged from 9.2°C to 15.2°C, with a mean temperature of 12.1 ± 1.4°C, while measured salinities ranged from 33.21 to 34.34, with an average of 33.73 ± 0.25 (Table 1). Both SST and salinity were correlated to an UI (average of 3 days prior to date of sampling) from NBDC station 46042 ($R^2 > 0.48$, $p < 0.0001$). The spring transition, marking the onset of coastal upwelling, was clearly reflected in the

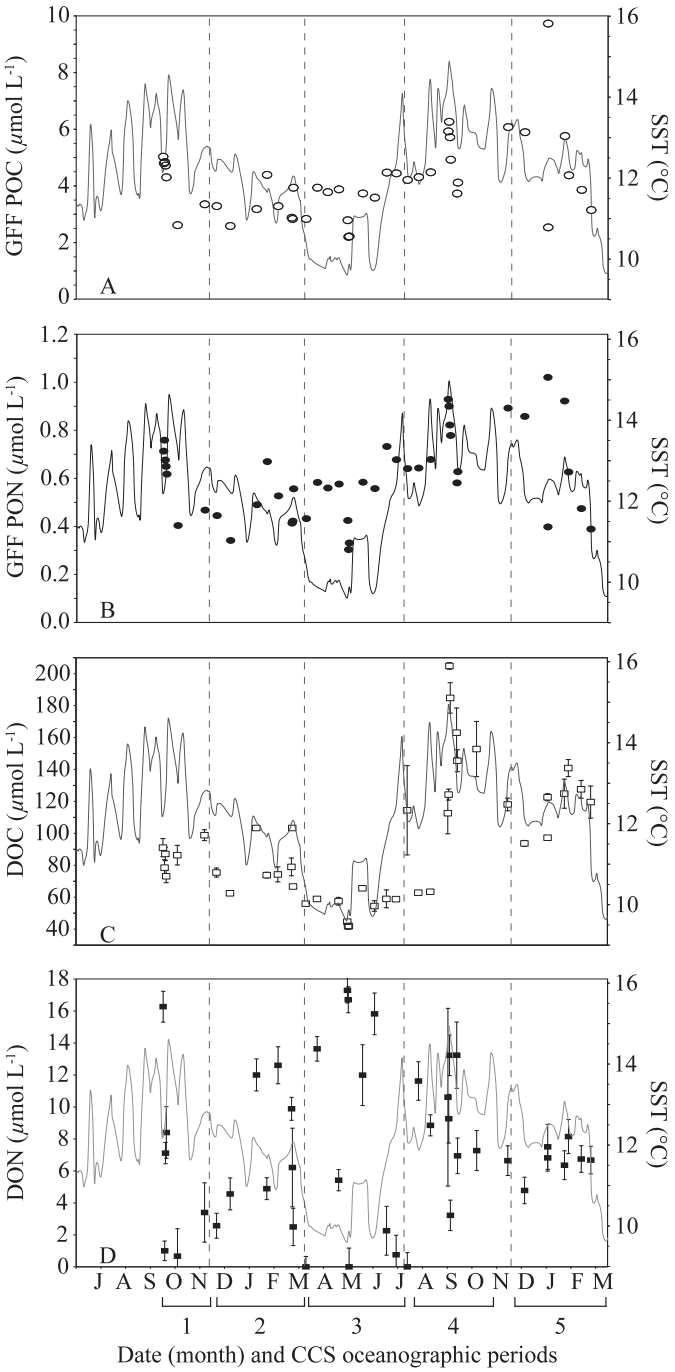

Fig. 3. The interseasonal variability of detrital organic matter pools is shown for the GCMPSL time series. (A–D) Gray lines represent SST (3-day moving average). Vertical dashed lines denote CCS oceanographic periods (1–5) as described in the Results. (A,B) Error is smaller than the size of the symbols. 18 October 2008 POC and PON data not shown. (C,D) Error bars represent the 1 σ standard deviation of $n = 3$ sample analyses.

physical data (Fig. 2C,D); SST dropped quickly from 12.0°C to 9.7°C over a period of ~ 1 week in early March 2008, and low SST waters persisted during the spring and summer months. Distinct SST and salinity trends were also observed in both winter and summer months. Analysis of water mass diffusive stability via "spiciness" (Munk 1981; Table 1) suggests that surface waters sampled at the GCMPSL during the "Upwelling" period are consistent with values reported from ~ 50 m depth, within the California Undercurrent (π = 0.3–0.4; Pierce et al. 2000; Flament 2002). Finally, the influence of freshwater sources (via nearby ephemeral drainages) was negligible at this site.

Similar seasonal offsets were observed for nutrient concentrations (Fig. 2E,F), which were also strongly correlated to physical properties. Nitrate, phosphate, silicic acid, and ammonium concentration ranges were 3.2–31.5 μmol L^{-1}, 0.2–1.4 μmol L^{-1}, 4.8–34.9 μmol L^{-1}, and 0.6–8.1 μmol L^{-1}, respectively (Table 1). The highest nutrient concentrations generally occurred during the upwelling season. During the winter and summer periods, nutrient concentrations were variable but lower than during the spring upwelling period ($\leq$ 15 μmol L^{-1} nitrate and silicic acid, and $\leq$ 0.8 μmol L^{-1} phosphate). Measured nitrate and silicic acid concentrations were both correlated to SST and salinity ($R^2 \geq 0.32$, $p \leq 0.0004$), whereas phosphate and ammonium were only significantly correlated to SST ($R^2 \geq 0.12$, $p \leq 0.0415$). With the exception of ammonium, all nutrient species were significantly correlated to water mass density (σ_t; $R^2 \geq 0.46$, $p < 0.0001$ for nitrate and silicate, and $R^2 = 0.12$, $p = 0.0278$ for phosphate) and 3 day averaged UI ($R^2 \geq 0.33$, $p < 0.0001$ for nitrate and silicate, and $R^2 = 0.11$, $p = 0.0250$ for phosphate).

Together, the changes we observed in water mass properties are consistent with classically defined CCS oceanographic periods (e.g., "Upwelling," "Oceanic," and "Davidson" periods; Skogsberg 1936; Skogsberg and Phelps 1946; Pennington and Chavez 2000). In this study (and subsequent figures), we described these as: (1) the "Oceanic 2007" period, from mid-September to mid-October 2007; (2) the winter "Davidson 2007" period, from mid-October 2007 to early March 2008; (3) the spring and summer "Upwelling 2008" period, from mid-March to early July 2008; (4) the "Oceanic 2008" period, from late July to mid-October 2008; and (5) the "Davidson 2008" period, from late November 2008 to mid-March 2009. Binning our data into these periods allows for a simplified overview of main trends and also offers a clear framework to directly compare our results to those reported from other CCS upwelling systems.

DOM and POM: Abundance, elemental and isotopic composition—A summary of average DOM and POM abundance and elemental and isotopic composition from main CCS periods is provided in Table 2. Except for one sample date, carbon and nitrogen concentrations of GF/F-POM (0.7–500 μm) at GCMPSL were low, ranging from 2.2 μmol L^{-1} to 9.7 μmol L^{-1} and 0.3 μmol L^{-1} to 1.02 μmol L^{-1} for POC and PON, respectively (Fig. 3A,B). The lowest POC and PON concentrations occurred during the Davidson 2007 and Upwelling 2008 periods (POC $<$ 3.4 μmol L^{-1}, PON ~ 0.5 μmol L^{-1}), whereas the highest values occurred during Oceanic periods and also the Davidson 2008 period (POC $>$ 4.2 μmol L^{-1}, PON $>$ 0.6 μmol L^{-1}). GF/F-POC and GF/

F-PON were significantly correlated to seawater physical properties (SST, salinity, and σ_t; $R^2 \geq 0.13$, $p \leq 0.03$) and to an average coastal UI (3 days prior to sample date; $R^2 \geq 0.26$, $p \leq 0.0004$). Despite the range in GF/F-POM C : N ratios during the time series ($\sim$ 5.2 to 8.2), GF/F-POC vs. GF/F-PON was very strongly correlated ($R^2 = 0.99$, $p < 0.0001$). In general, high C : N GF/F-POM occurred during the Oceanic and Davidson periods (C : N $\sim$ 6.6–7.4) and lower C : N GF/F-POM during the Upwelling 2008 period (C : N $\sim$ 6.6).

Ultrafiltered POM (UPOM; 0.1–100 μm) average C and N concentrations followed patterns similar to GF/F-POM throughout all CCS ocean periods, indicating that the production and cycling of large vs. small POM size classes both follow similar seasonal changes. On average, UPOM C : N ratios (7.1 $\pm$ 0.4; $n = 10$) were slightly higher than those of GF/F-POM (6.8 $\pm$ 0.6; $n = 44$) and also during CCS periods, with only one similar C : N ratio observed during the Oceanic 2008 period. GF/F-POM C : N ratios also followed trends of total POC and PON concentrations during CCS periods. However, UPOM C : N ratios had the opposite trend, with the highest C : N ratio observed during the Upwelling 2008 period (Table 2).

DOC and DON ranged from 42 μmol L^{-1} to 205 μmol L^{-1} and 0 μmol L^{-1} to 17.3 μmol L^{-1}. Average DOC and DON concentrations for the time series were 94 $\pm$ 39 μmol C L^{-1} and 7.5 $\pm$ 4.9 μmol N L^{-1}, respectively ($n = 42$; Fig. 3C,D). The lowest average DOC values occurred during the Upwelling 2008 period ($\sim$ 54 μmol L^{-1}, $n = 10$) and the highest values during the Oceanic periods (86–133 μmol L^{-1}). DOC was significantly correlated to POM abundance (POC and PON; $R^2 \geq 0.18$, $p \leq 0.0046$), seawater physical properties (SST, salinity, σ_t; $R^2 > 0.34$, $p < 0.0002$), and also to UI ($R^2 > 0.19$, $p < 0.003$). In contrast, DON was not significantly correlated to either seawater physical properties or to POM (POC and PON) abundance. In addition, there was no correlation between DOC and DON concentrations ($R^2 = 0.002$, $p = 0.807$). However, (with the exception of ammonium) DON was significantly correlated ($p \leq 0.0025$) to major nutrient species measured during the time series ($R^2 = 0.31$, 0.42, and 0.21 for nitrate, phosphate, and silicate, respectively); the highest DON (10–17 μmol L^{-1}) consistently occurred during nutrient-depleted conditions (nitrate < 15 μmol L^{-1}), whereas the lowest DON (< 5 μmol L^{-1}) occurred at nitrate values > 15 μmol L^{-1}.

DOM C : N ratios had an average range of $\sim$ 8–18 during CCS periods (Table 2). While there was no statistical difference between average DOM C : N ratios between any two CCS periods (Student's t-test), they displayed a trend similar to that of GF/F-POM. The lowest and highest average DOM C : N seasonal averages coincided with the Upwelling 2008 and Oceanic/Davidson periods, respectively. Average HMW DOM C : N ratios (9.5 $\pm$ 0.9, $n = 11$) were both lower and less variable than total DOM C : N ratios. Like total DOM, there was no statistical difference between HMW DOM C : N ratios between any two CCS periods. Qualitatively, however, we note that the seasonal offsets in average HMW DOM elemental ratios were identical to those observed for total DOM. Results from linear regression analyses indicate robust correlations between HMW DOM C : N to both physical properties (SST, σ_t, 3 day UI; $R^2 \geq 0.41$, $p \leq 0.0325$) and to POM C and N pools (GF/F-POM $R^2 \geq 0.39$, $p \leq 0.0387$; UPOM $R^2 \geq 0.68$, $p \leq 0.0064$).

GF/F-POM δ^{13}C and δ^{15}N values were variable, with δ^{13}C ranging between -25.2‰ and -17.7‰ and δ^{15}N between +3.5‰ and +9.7‰. However, average δ^{13}C and δ^{15}N values for the time series had small standard deviations (GF/F-POM average δ^{13}C -22.0 ± 1.1‰, GF/F-POM average δ^{15}N value +5.9 $\pm$ 1.3‰). With the exception of the Oceanic 2008 period, there was no significant difference between GF/F-POM δ^{13}C and δ^{15}N values between any two CCS periods (Student's t-test), suggesting similar isotopic sources during the time series. The positive δ^{13}C and δ^{15}N values from the Oceanic 2008 period (Table 2) appear to be outliers—similar to kelp end members for the Big Sur region (Foley and Koch 2010). Therefore, we exclude Oceanic 2008 CCS average period data from further discussion. The UPOM isotopic signatures display more seasonal variability vs. GF/F-POM. UPOM δ^{13}C and δ^{15}N values ranged from -17.0‰ to -22.5‰ and +3.1‰ to +6.5‰, respectively. On average, UPOM was heavier for δ^{13}C (-21.2‰ $\pm$ 1.1‰) and lighter for δ^{15}N (+4.1‰ $\pm$ 0.8‰) than for GF/F-POM δ^{13}C and δ^{15}N values, respectively. The offset in δ^{13}C between small vs. large POM falls just outside the 95% confidence interval ($p = 0.12$). The offsets between small vs. large POM δ^{15}N values (UPOM = +4.1‰ $\pm$ 0.8‰ vs. GF/F-POM = +5.9‰ $\pm$ 1.3‰) were statistically significant (t-test, $t = 2.0$, df = 16.3, $p = 0.0011$).

HMW DOM δ^{13}C and δ^{15}N values ranged from -17.5‰ to -21.3‰ and +3.5‰ to +7.3‰, respectively. For δ^{15}N, there were no statistically significant differences among CCS periods. For δ^{13}C (again with the exception of the Oceanic 2008 period, which again trended toward a kelp end member), only the HMW DOM δ^{13}C signatures from the Davidson 2007 and Oceanic 2007 periods were statistically different ($p \leq 0.0297$). The average HMW DOM δ^{13}C value (-20.4‰ $\pm$ 0.8‰) from all periods (excluding Oceanic 2008) is very similar to expected open ocean values (-21‰ to -22‰; Benner et al. 1997). In contrast, the average δ^{15}N value for HMW DOM (+5.7‰ $\pm$ 1.2‰) was depleted in comparison to open ocean values reported by Benner and co-workers (1997; +7‰ to +8.5‰); however, it was similar to the HMW DOM δ^{15}N value reported by Meador et al. (2007) for both coastal and open Pacific Ocean (stations: CalCOFI = +6.1‰, Scripps pier = +5.8‰, MP9 = +5.4‰ $\pm$ 0.7‰).

Discussion

POM abundance and elemental ratios: Implications for plankton growth and limiting nutrients—POC abundance was far lower than that reported for other regional upwelling centers, including nearby Monterey Bay (3–40 mmol L^{-1} C; Bac et al. 2003) and the Oregon coast (37 $\pm$ 5 μmol L^{-1} C; Hill and Wheeler 2002). The one observed event of high POC and PON concentrations (18 October 2008; 29.4 μmol L^{-1} POC and 4.1 μmol L^{-1} PON) can

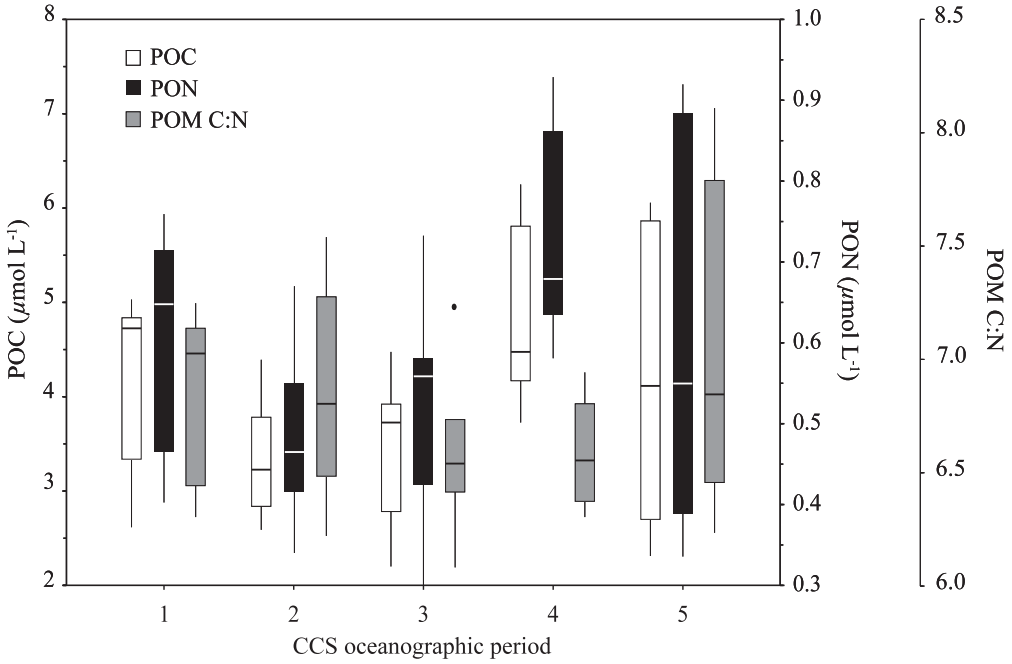

Fig. 4. Averaged POM concentrations and elemental ratio quantiles are shown for CCS periods. Numbered CCS oceanographic periods (1–5) are as described in the Results. Box boundaries indicate the 25th and 75th percentiles of sample population distributions (thin vertical line), horizontal line indicates the median, whiskers the 10th and 90th percentiles, and dots the sample outliers.

most likely be attributed to a phytoplankton bloom in the Monterey Bay during this time period, which was then advected around the Monterey Peninsula and south along the Big Sur coastline (R. Kudela pers. comm.). Since other POC and PON concentrations observed during the time series do not appear to be influenced by large blooms (and therefore better reflect typical oceanographic variability at this site), we exclude values from 18 October 2008 in our compiled data for CCS oceanographic periods.

The correlation we observe between both GF/F-POC and GF/F-PON concentrations to physical data and water mass properties (UI, SST, salinity, and σ_t) suggests that advected suspended POM also exerts an influence on POM abundance and composition. While POC and PON follow similar trends (Fig. 4), the seasonal differences are quite different from those expected in more productive upwelling areas. For example, during a time series $\sim$ 9 km offshore from Newport Oregon, Hill and Wheeler (2002) observed highest POC and PON concentrations (36 μmol L^{-1} and 5 μmol L^{-1}, respectively) during periods of intense coastal upwelling, a trend opposite to that we observed. Both in our study and that of Hill and Wheeler (2002), the lowest POM C : N ratios occur during coastal upwelling, while high POM C : N ratios occur during periods of warming/stratification (Fig. 4). Therefore, the trends we observe are consistent with chemically ''fresh'' (N-rich) POM produced during coastal upwelling, and more C-rich (and possibly more degraded) POM persisting during periods of relatively greater water-column stratification.

Elemental ratios of suspended POM and nutrients can also help constrain phytoplankton growth status and limiting nutrients in the water column. As noted above, GF/F-POC was significantly correlated to GF/F-PON during the time series ($R^2 = 0.99$, $p < 0.0001$). The slope of this model II regression (7.28) indicates that phytoplankton C and N approximate Redfield proportions at this site (Table 3). Slopes of nutrient regressions (nitrate, silicate) relative to phosphate (Table 3) are elevated with respect to Redfield conditions, with a N : P slope = 20.0 and a Si : P slope = 21.9. The regression slope of Si : N (1.10) indicates uptake of silicate over nitrate, consistent with previous Si : N ratios reported from upwelling systems of the Oregon coast (Hill and Wheeler 2002). Together with POC and PON results, these relationships yield a C : N : Si : P ratio of 146 : 20 : 21 : 1. Finally, within the present study, y-intercepts of geometric mean Model II regressions (Table 3) suggest the order of limiting nutrients to be Si > N > P in this upwelling system.

Overall, the POM concentrations and elemental ratios we observe are consistent with limited phytoplankton biomass in this upwelling system, in direct contrast to the high productivity observed in other CCS upwelling systems. Many possible physical/biological controls on phytoplankton may contribute to the low POM concentrations we observe. For example, zooplankton grazing pressure and mixing/advection can readily limit population growth (Smayda 1997). The strong physical forcing by winds and constant horizontal offshore advection at the GCMPSL is therefore one factor likely limiting phytoplankton biomass. Another possibility is micronutrient (iron) limitation. Iron-deplete conditions have been reported for the Big Sur coastline (Bruland et al. 2001). While we did not measure iron concentrations in this study, the elevated Si : N ratio we observe is consistent with previous observations of

Table 3. Redfield molar ratios (by atom) are given for measured seawater nutrient (nitrate, silicate, and phosphate), suspended large POM (GF/F-POM), suspended small POM (UPOM), and high-molecular-weight (HMW) DOM concentrations. The slopes of a linear regression determine Redfield ratios. *n*, sample populations.

Redfield ratio	*n*	y-intercept	±	slope	±	*p* value	R^2
POM C : N	44	−0.27	0.12	7.28	0.13	<0.0001	0.9859
Nutrient N : P	44	−0.65	1.53	20.02	1.99	<0.0001	0.6285
Nutrient Si : P	44	−1.80	2.00	21.94	2.59	<0.0001	0.5003
Nutrient Si : N	44	−1.09	0.75	1.10	0.05	<0.0001	0.9134
UPOM C : N	10	−0.02	0.09	5.59	0.50	<0.0001	0.6871
HMW DOM C : N	11	−0.37	0.69	11.77	1.08	<0.0001	0.9253
POM C : N : Si : P	146 : 20 : 21 : 1						
UPOM C : N : Si : P	112 : 20 : 21 : 1						

preferential silicate uptake over nitrate under iron-deplete conditions on the Big Sur coast (Hutchins and Bruland 1998). Overall, while our data cannot definitively identify mechanisms limiting POM abundance (i.e., iron limitation vs. mixing/advection), our data are consistent with this CCS upwelling system as an HNLC region.

DOM variability, elemental ratios, and production estimates—Observed ranges in DOC and DON (42–205 μmol L^{-1} and 0–17.3 μmol L^{-1}, respectively) are generally consistent with those reported by Hill and Wheeler (2002) for an upwelling center time series on the Oregon coast (DOC ~ 45–180 μmol L^{-1}; DON ~ 4–15 μmol L^{-1}). The significant correlation of DOC to POM abundance suggests that DOC concentrations are directly linked to biological production during periods of high SST and water-column stratification. However, the observation that DOC was also more strongly correlated to seawater physical properties than POC indicates that physical mixing also exerts a large control on DOC abundance. This is consistent with upwelling of low DOC water to the surface, coupled with limited phytoplankton biomass.

In contrast, the lack of correlation between DON and seawater physical properties (or DOC, POC, and PON abundance) indicates that DON cycling is fundamentally decoupled from both the DOC pool and primary production (i.e., POM). While this may seem unexpected, previous studies have shown similar results for coastal and open ocean environments (Hansell et al. 1993; Hansell and Carlson 2001; Hill and Wheeler 2002). For example, concomitant increases in DON as a function of decreasing nitrate values have been observed on transects across the equatorial upwelling zone in the Pacific Ocean (Hansell and Waterhouse 1997; Libby and Wheeler 1997; Raimbault et al. 1999). This was attributed to new production from upwelled equatorial nitrate and then subsequent algal DON exudation during advection to nutrient-deplete higher latitudes. However, given the trends in DON abundance we observe at the GCMPSL, advected sources of DON seem unlikely. Instead, our data suggest enhanced in situ DON production under nutrient-deplete and elevated light conditions. Several possible mechanisms for this have been suggested in the literature, including active phytoplankton DON release in response to nutrient stress or elevated light conditions (Fogg 1983; Bronk and Ward 1999; Lomas and Glibert 1999) or passive release due to physiological stress, grazing pressure, and viral lysis (Bronk 2002). Overall, the decoupling of DON from both DOC and POM pools, together with robust correlations to nutrient concentrations, suggests that DON production within this HNLC upwelling region may also be attributed to nutrient availability.

Averaged DOC and DON concentrations from CCS periods (Fig. 5) summarize these observations and underscore the differences in DOM production/export in this system vs. that of more productive upwelling environments. The occurrence of low DOC during the Upwelling 2008 period and high DOC in the Oceanic periods differs greatly from observations within high-production upwelling zones—where high DOC concentrations typically occur during upwelling (Alvarez-Salgado et al. 2001*a*; Hill and Wheeler 2002). The decoupling of DON from DOC is also apparent in seasonally averaged data (Fig. 5). The lack of a correlation between DON values from CCS periods may be related to higher DON interseasonal variability, which would also be consistent with the fundamental decoupling of DOC and DON discussed above. For example, rapid turnover in the DON pool (on timescales of only a few days) has previously been documented for the Monterey Bay (Bronk and Ward 1999). Together these data suggest that the DON pool is extraordinarily dynamic relative to DOC.

Average DOM C : N ratios during CCS periods provide an alternate approach for assessing seasonal changes in DOM composition. Average DOM C : N ratios between CCS periods (Fig. 5) generally fall in between DOM C : N ratios reported for the open ocean (C : N ~ 13–14; Bronk 2002; Hopkinson and Vallino 2005) and coastal ocean (C : N ~ 17; Bronk 2002; Hill and Wheeler 2002). DOM C : N ratios display a similar seasonal trend to that of GF/F-POM, with the lowest and highest average DOM C : N seasonal values coinciding with Upwelling and Oceanic/Davidson periods, respectively. This differs from DOM C : N reported for the Oregon coast, where the highest DOM C : N values occurred during the upwelling period (C : N ~ 20) and the lowest DOM C : N values occurred during "winter" and "warming" periods (C : N of 12.0 and 8.4, respectively). N-rich DOM from this study and from Hill and Wheeler (2002) both have elemental ratios consistent with modeled C : N ratios of "labile" DOM in the global ocean (C : N ~ 9.95; Hopkinson and Vallino 2005), although occurring at different CCS periods.

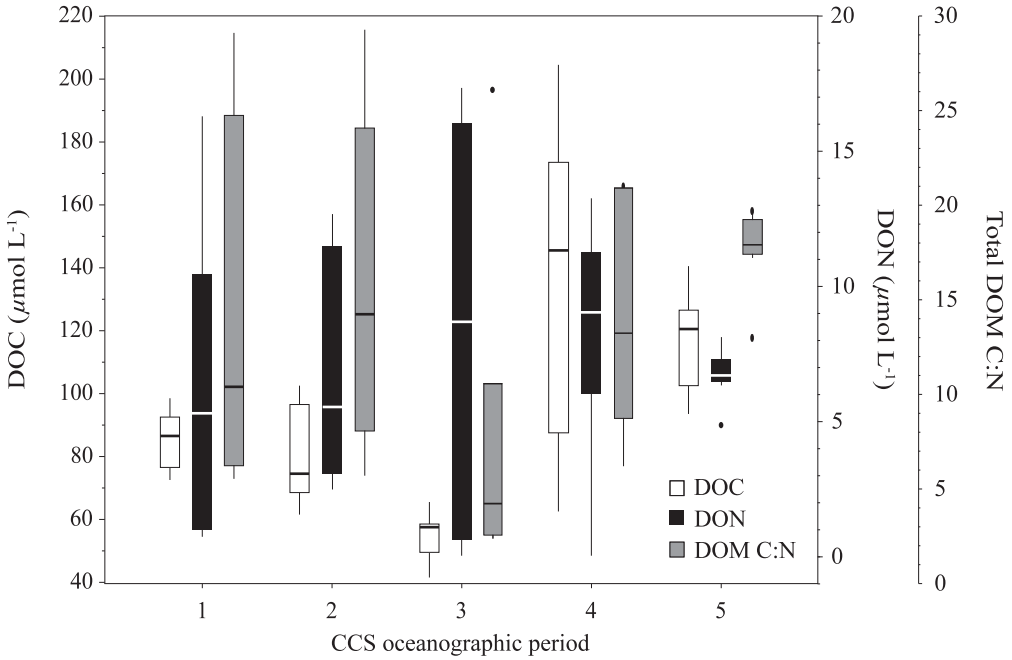

Fig. 5. Averaged DOM concentrations and elemental ratio quantiles are shown for CCS periods. Numbered CCS oceanographic periods (1–5) are as described in the Results. Box boundaries indicate the 25th and 75th percentiles of sample population distributions (thin vertical line), horizontal line indicates the median, whiskers the 10th and 90th percentiles, and dots the sample outliers.

Together, these seasonal trends in DOM abundance and elemental composition may have significant implication for the role of seasonal production and export of DOM from the CCS. By subtracting the average Upwelling 2008 DOC end member (54 μmol L^{-1}; Table 2) from that of the other CCS periods, we can estimate a net "excess" DOC production from 26 μmol L^{-1} to 30 μmol L^{-1} (or 0.27–0.62 μmol C L^{-1} d^{-1}) during the Oceanic and Davidson 2007 periods and from 64 μmol L^{-1} to 79 μmol L^{-1} (or 0.62–0.91 μmol C L^{-1} d^{-1}) during the Oceanic and Davidson 2008 periods. While regional changes in DOC concentrations have not been previously reported for the Monterey Bay or Big Sur region, these estimates are similar to DOC net production estimates made by Hill and Wheeler (2002) for the Oregon upwelling period ($\sim$ 62 μmol L^{-1}), suggesting that both of these upwelling regions produce similar amounts of DOC per annum, albeit during very different CCS oceanographic periods.

Finally, by using average DOM C : N ratios we can estimate excess DON production and potential export. For the Oceanic/Davidson 2007 CCS periods (DOM C : N = 13.9–15.5) excess DON ranges from 1.7 μmol L^{-1} to 2.3 μmol L^{-1} (or 0.017–0.024 μmol N L^{-1} d^{-1}), and excess DON estimates from the Oceanic/Davidson 2008 periods (DOM C : N = 17.8–18.2) range from 3.6 μmol L^{-1} to 4.3 μmol L^{-1} (or 0.037–0.045 μmol N L^{-1} d^{-1}). These estimates of excess DON are consistent with previously reported DON production rates for the Monterey Bay (average = 0.033 $\pm$ 0.038 μmol N L^{-1} d^{-1}; Bronk and Ward 1999; Ward and Bronk 2001). This excess DON is sizeable when compared to yearly average DON values, representing $\sim$ 28–33% of total DON from the Oceanic/Davidson 2007 periods and $\sim$ 51–54% of total DON from the Oceanic/Davidson 2008 periods. Overall, these results strongly support previous work highlighting the importance of DOM export from upwelling systems in supplementing offshore/mesopelagic ecosystems (Alvarez-Salgado et al. 2001*b*; Hill and Wheeler 2002; Nieto-Cid et al. 2004).

Size-fractionated POM: Composition, sources, and cycling—The possible linkage between DOM and POM size to chemical composition has never been examined for a coastal upwelling region. Because physical transport mechanisms are strongly tied to OM size (i.e., sinking vs. suspended POM and DOM), variations in OM size vs. composition could have considerable implications for OM export from upwelling regions. To our knowledge, this is the first study to examine contemporaneous bulk elemental and isotopic variation of both POM and DOM size classes.

The observation that the average UPOM C : N ratios were slightly higher than those of GF/F-POM (Fig. 6A) suggests that during the upwelling CCS period larger POM is generally N rich, whereas smaller POM is more C rich. This offset is consistent with "size reactivity" continuum ideas (Amon and Benner 1994; Amon and Benner 1996), suggesting that within this upwelling region larger POM may be N rich and chemically "fresher," whereas smaller C-rich POM may comprise more chemically degraded material, following the general trend observed in most detrital OM (Cowie and Hedges 1994). This interpretation is also consistent with the older ^{14}C age of suspended vs. sinking POM observed in many ocean regions (Druffel

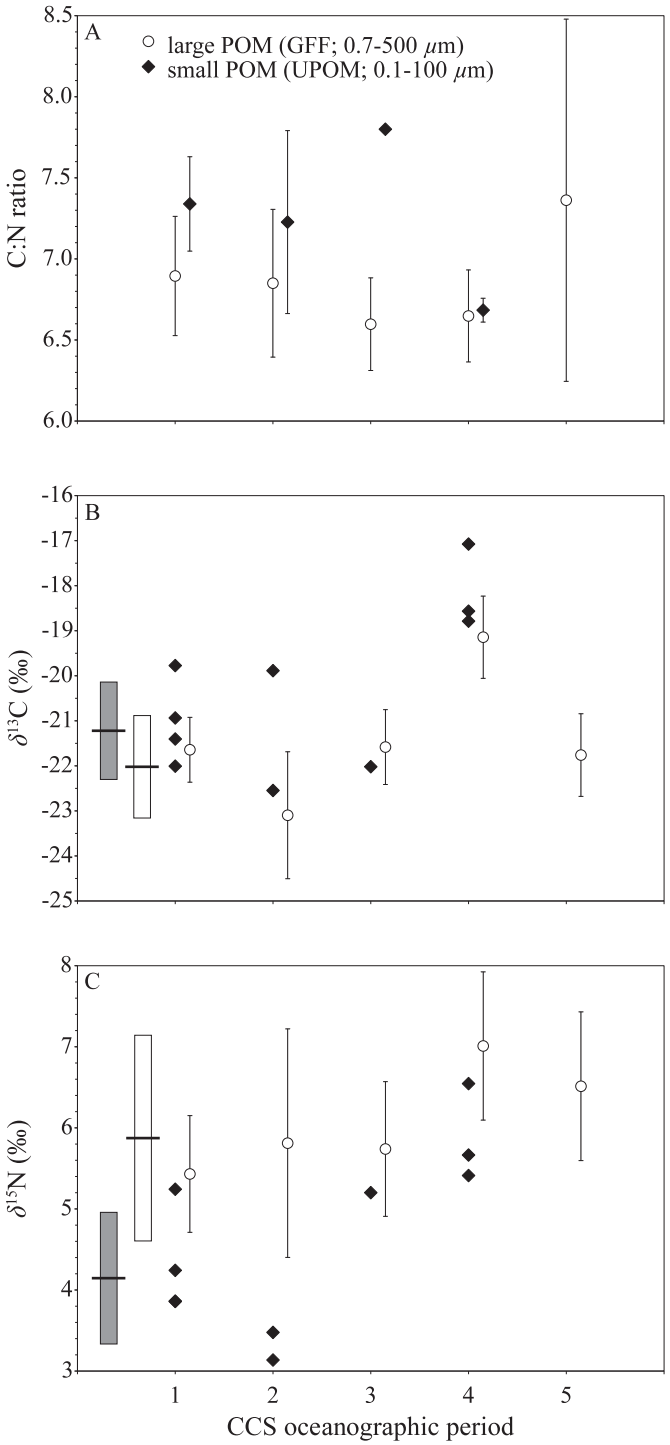

Fig. 6. The elemental and stable isotopic composition is shown for large (GF/F) vs. small (UPOM) suspended particles during CCS periods. All symbols are as in (A). Errors are 1 σ standard deviations reported in Table 2. (B,C) Solid black horizontal bars represent the average δ^{13}C and δ^{15}N values from all CCS periods (excluding the Oceanic 2008 period). Gray and open rectangles represent small and large POM standard deviations of averages. Numbered CCS oceanographic periods (1–5) are as described in the Results.

et al. 1992). However, while the overall UPOM C : N range we observe is similar to that reported for the open ocean, we also note that C-rich UPOM is not typical in the open ocean (Benner et al. 1997; Sannigrahi et al. 2005; Roland et al. 2009). While we cannot provide a direct explanation, it seems that different POM sources in the coastal vs. open oligotrophic ocean are likely responsible.

The offsets observed in stable isotopic (δ^{13}C and δ^{15}N) signatures of small vs. large POM (Fig. 6B,C) strongly suggest that different POM size classes may also have characteristically different sources. Overall, the GF/F-POM δ^{13}C and δ^{15}N values are consistent with previous studies of POM from the Monterey bay region (Rau et al. 1990). Average GF/F-POM δ^{13}C (-22.0 ± 1.1‰; Fig. 6B) again indicates that marine phytoplankton are the primary source of the larger suspended POM fraction throughout all periods. The observation that UPOM is on average isotopically enriched (-21.2‰ $\pm$ 1.1‰; Fig. 6B) relative to GF/F-POM is also consistent with previously observed δ^{13}C offsets in the open ocean (Druffel et al. 1996; Sannigrahi et al. 2005; Roland et al. 2009). Several possibilities have been suggested to explain this size-related δ^{13}C offset, including: (1) the influence of sub-micron aeolian particles in smaller POM with lighter carbon signatures (δ^{13}C = -26.5‰ to -26.7‰; Chesselet et al. 1981); (2) changes in relative terrestrial OM contribution (Hernes and Benner 2002); or (3) fundamental differences in stable isotopic fractionation between small vs. larger marine unicellular organisms, such that POM size fractions may reflect differences in primary producer community composition (i.e., eukaryotic vs. prokaryotic; Close et al. 2011; A. Pearson pers. comm.). This last possibility would also be consistent with higher rates of carbon-specific photosynthesis of larger vs. smaller coastal phytoplankton cells observed within upwelling systems (Cermeno et al. 2005). We also note that an increased terrestrial/aeolian contribution to UPOM would lead to lighter δ^{13}C values, the opposite of what we observe. Finally, a simple isotopic mass balance indicates that material *not* recovered in the UPOM fraction has a similar marine δ^{13}C signature (-21.9‰ $\pm$ 1.5‰), suggesting that the isolation process itself does not selectively exclude an isotopically distinct source contribution.

Average GF/F-POM δ^{15}N (+5.9‰ $\pm$ 1.3‰) was lower than previously reported nitrate δ^{15}N values from the Monterey Bay (+7‰ to +8‰; Altabet et al. 1999), likely due to incomplete nitrate utilization in this system. The significant δ^{15}N offset between larger vs. smaller suspended POM (Fig. 6C; +4.1‰ vs. +5.9‰) would seemingly suggest that smaller POM is sourced from lower trophic position material (i.e., proportionally less microzooplankton and/or higher trophic position organisms isolated in UPOM). However, recent work has suggested an alternate hypothesis—that these δ^{15}N offsets might be attributed to the differential size and metabolism of unicellular organisms.

A recent study from the Sargasso Sea observed consistently lighter δ^{15}N prokaryotes (both heterotrophic and cyanobacteria) vs. heavier δ^{15}N small ($\leq$ 30 μm) eukaryotes, resulting in large δ^{15}N offsets ($>$ 3‰)

throughout the euphotic zone (Fawcett et al. 2011). This suggests that an analogous explanation may exist for both $\delta^{13}C$ and $\delta^{15}N$ offsets in small vs. large POM fractions. Finally, we note that in the open sea, degradation of suspended POM typically increases $\delta^{15}N$ values (Altabet 1988). However such a signal has never been documented from suspended POM in a coastal upwelling system, and the magnitude of this effect is unknown. While some influence of degradation would be expected based on C : N data (and expected ^{14}C ages), our results suggest that, with respect to $\delta^{15}N$, a degradation effect is likely masked by differential N sources.

Overall, these observations represent an extensive data set documenting characteristic offsets in both elemental and isotopic values with particle size in the ocean—together suggesting that both degradation and differential POM sources may play important roles. The data indicate that, while all POM size fractions are of marine origin, elemental compositions are linked to degradation and isotopic signatures largely reflect POM sources—perhaps based on small vs. large size classes of organisms ultimately incorporated into these POM pools. Neither isotopic nor elemental data suggests an important contribution of terrestrial material to POM size fractions.

Size-fractionated DOM: Composition, sources and cycling—On average, HMW DOM C : N ratios (9.5 ± 0.9) are substantially lower than previously reported open ocean HMW DOM C : N (C : N ≥ 16; Benner et al. 1997). This observation highlights important differences in HMW DOM chemical composition between this upwelling region and the open ocean, with coastal HMW DOM containing more nitrogenous compounds (e.g., protein or amino sugar) vs. C-rich surface open ocean HMW DOM (e.g., high in carbohydrates; Benner et al. 1992; Kaiser and Benner 2009). While no statistical difference was found between average seasonal HMW DOM C : N, qualitatively we note that for both HMW DOM and total DOM the most N-rich material was observed during the Upwelling 2008 period, while the most C-rich HMW DOM was observed during the Oceanic and Davidson periods (Fig. 7A).

The presence of N-rich total and HMW DOM during coastal upwelling is the opposite of what one might expect based purely on physical mixing (i.e., upwelling of deep C-rich DOM; Benner et al. 1997; Hopkinson and Vallino 2005). Instead, these results indicate that the chemical composition of both HMW and total DOM pools results from enhanced DON production during upwelling and higher relative production of DOC during oceanic periods (i.e., warmer, stratified water columns producing more carbohydrate-enriched DOM; Williams 1995; Alvarez-Salgado et al. 2001*a*; Goldberg et al. 2009). Results from linear regression analyses support this idea, with robust correlations between HMW DOM C : N to both physical properties (SST, σ_t, 3-day UI; $R^2 \geq 0.41$, $p \leq 0.0325$) and also to POM C and N pools (GF/F-POM $R^2 \geq 0.39$, $p \leq 0.0387$; UPOM $R^2 \geq 0.68$, $p \leq 0.0064$). Together, these results indicate that while physical processes clearly contribute to HMW DOM chemical composition (via

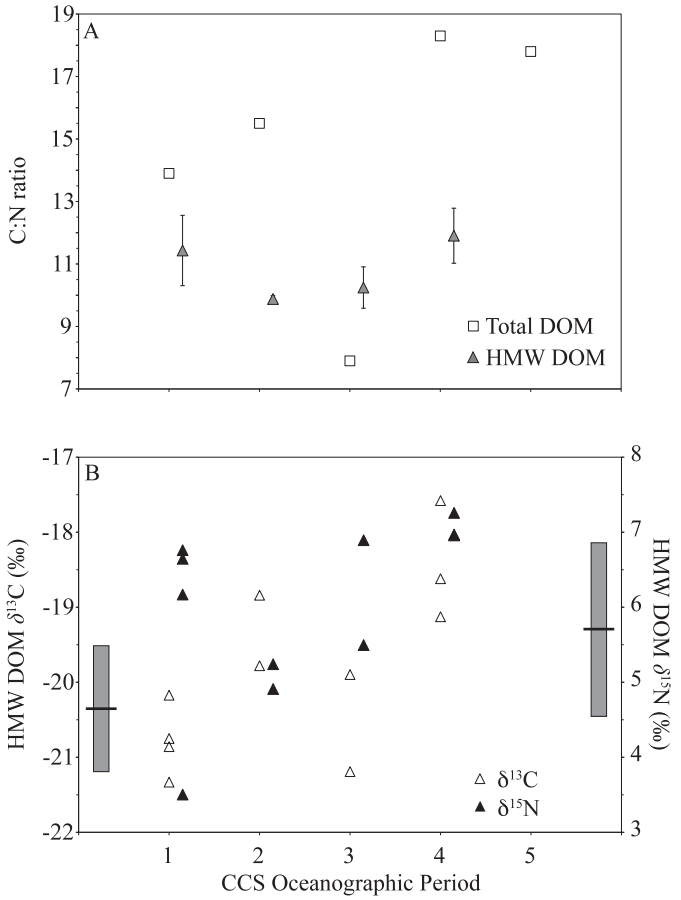

Fig. 7. The elemental and stable isotopic composition of high-molecular-weight (HMW) DOM is shown for CCS periods. (A) HMW DOM error bars represent the 1 σ standard deviation. C : N errors for total DOM values are reported in Table 2. (B) Black horizontal bars with gray vertical rectangles represent the average and standard deviation of $\delta^{13}C$ (left) and $\delta^{15}N$ (right) values from CCS periods (excluding the Oceanic 2008 period). Numbered CCS oceanographic periods (1–5) are as described in the Results.

physical mixing and advection of existing DOM pools), overlaid on this signature is the significant influence of local HMW DON production. Our results indicate that the HMW DOM produced in this coastal region contains > 40% more nitrogen than open ocean HMW DOM. The advection of this N-rich HMW DOM may represent an important mechanism for labile ON export to adjacent oligotrophic and mesopelagic ecosystems.

A key advantage to isolating ultrafiltered (i.e., HMW) DOM is that it allows for the direct measurement of stable isotopes ($\delta^{13}C$ and $\delta^{15}N$), which are extremely difficult to make for total DOM when significant quantities of DIN are present (Meador et al. 2007; Knapp et al. 2011). Average HMW DOM $\delta^{13}C$ (−20.4‰ ± 0.8‰) from all periods (Fig. 7B; excluding Oceanic 2008) is similar to open ocean values (−21‰ to −22‰; Benner et al. 1997), consistent with our interpretation of phytoplankton as a DOM source. Average HMW DOM $\delta^{15}N$ (+5.7‰ ± 1.2‰) was depleted in comparison to open ocean values (+7‰ to +8.5‰) reported by Benner et al. (1997), but similar to

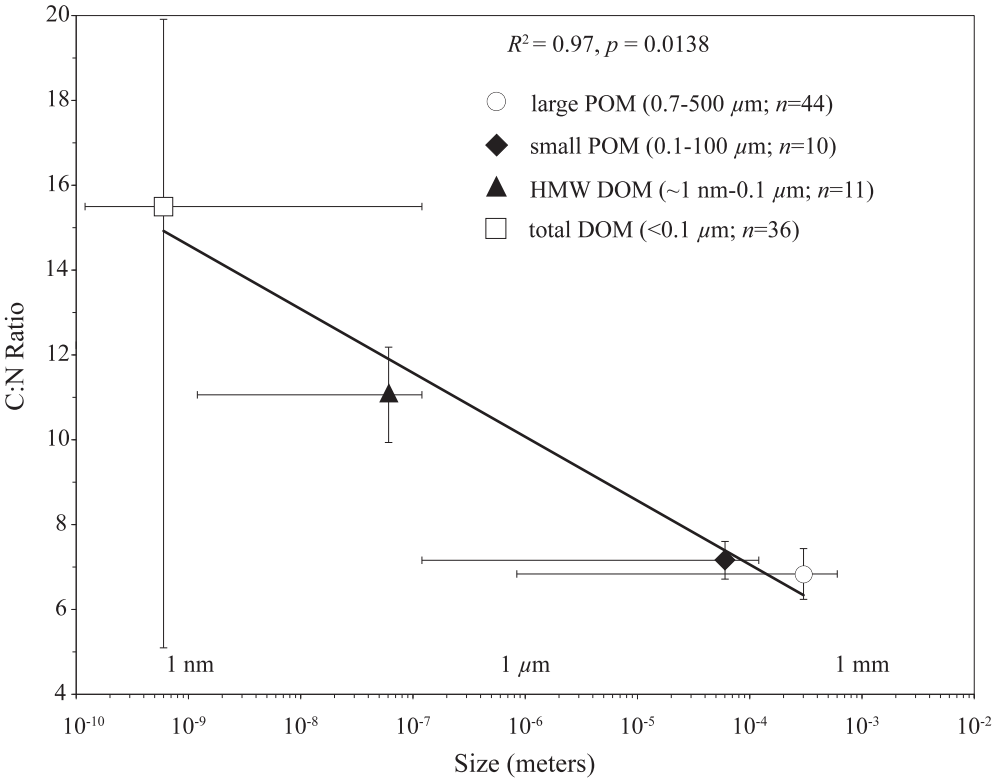

Fig. 8. A summary of size vs. elemental composition is shown for detrital organic matter size fractions. Horizontal error bars represent the total size range (x-axis) of organic matter pool size classes. With the exception of total DOM, sample sizes represent the middle of operationally defined size classes. In the case of total DOM (< 0.1 μm) an average size of 500 daltons was assigned (i.e., primarily low-molecular-weight DOM). Vertical error bars represent the 1 σ standard deviation of organic matter C : N ratio (y-axis). Thick black line depicts the logarithmic (ln x) regression analysis.

oceanic values reported by Meador et al. (2007; ~ 5.4‰ ± 0.7‰) and also two HMW DOM δ^{15}N measurements from the California coast (CalCOFI = +6.1‰ and Scripps pier = +5.8‰; Meador et al. 2007). However, the range of HMW DOM δ^{15}N we observe (+3.5‰ to +7.3‰) is substantially larger than has been previously reported, indicating dynamic HMW DON cycling in this upwelling system.

Overall, δ^{13}C and δ^{15}N signatures are consistent with HMW DOM as the most labile DOM component (Amon and Benner 1994; Walker et al. 2011). The similarity between average isotopic signatures of HMW DOM and POM also suggest a direct linkage between DOM and phytoplankton biomass. HMW DOM δ^{13}C and δ^{15}N (δ^{13}C = −20.4‰ ± 0.8‰, δ^{15}N = +5.7‰ ± 1.2‰) are statistically identical to the large POM fraction (δ^{13}C = −22.0‰ ± 1.1‰, δ^{15}N = +5.9‰ ± 1.3‰). HMW DOM and POM δ^{15}N were correlated, but they fell just outside the 90% confidence interval (R^2 = 0.23, p = 0.13). Combined with strong correlations between HMW DOM and POM C : N ratios mentioned above, these results further indicate local phytoplankton as a primary source of HMW DOM. This is also consistent with previous work noting that the δ^{15}N signatures of HMW DON closely reflect local oceanographic processes and N sources, as opposed to material derived from higher trophic positions (Benner et al. 1997; Bronk 2002).

The similar HMW DOM and POM δ^{15}N values (depleted vs. expected local nitrate) are consistent with incomplete nitrate utilization for this upwelling region and with recent compound-specific isotopic studies (McCarthy et al. 2004; McCarthy et al. 2007), indicating relatively little heterotrophic degradation in HMW DOM amino acids. However, previous open ocean studies have observed high D/L amino acid ratios in HMW DOM (McCarthy et al. 1998; Kaiser and Benner 2008), suggesting a prokaryotic source. It is important to note that these observations are not contradictory. For example, in the open ocean cyanobacterial biomass may represent a major source of fresh DON, while in coastal upwelling systems this is unlikely. Future comparisons of D/L signatures of DON in upwelling regions may be useful in understanding the relative influence of autotrophic vs. heterotrophic bacteria in the production of oceanic DON. Finally, the observation that HMW DOM and large POM isotopic values are offset from small POM (UPOM; Fig. 6B,C) suggests that the source and degradation state of labile POM and DOM pools may be different in coastal upwelling systems vs. offshore regions.

A size vs. elemental composition continuum of detrital OM pools—Previous work has shown that the size of detrital OM is strongly linked to its reactivity—where larger OM size fractions are chemically "fresh," are more bioavailable, and have faster turnover rates (Amon and Benner 1994; Benner et al. 1997; Sannigrahi et al. 2005). The elemental compositions of all OM size fractions examined here are consistent with size–reactivity continuum ideas and range from high C : N in total DOM to low C : N in large POM. Analogous relationships between C : N ratio and degradation state have previously been observed within DOM, suspended vs. sinking POM, and also marine sediments (Cowie and Hedges 1994; Loh and Bauer 2000; Hopkinson and Vallino 2005). However, an explicit relationship between relative OM size and C : N ratio has never been examined across both DOM and POM pools. Figure 8 summarizes the relationship between OM elemental composition and size (ln size) for all OM pools measured and demonstrates a robust correlation (R^2 = 0.97, p = 0.0138).

The presence of a clear relationship across a wide range in OM size, linking DOM and POM, is both striking and somewhat unexpected. There are numerous possible sources of DOM (e.g., phytoplankton exudation, viral lysis, etc.; Bronk 2002; Carlson 2002). However, this result suggests that a continuous "precursor–product" style relationship exists between plankton biomass in both POM size classes and subsequently to DOM size classes, presumably via degradation. This observation further suggests that, at least in this upwelling region, the relationship between detrital OM size and nitrogen content can be quantifiably predicted. To our knowledge, this represents the first evidence of a *quantifiable* "size–reactivity" relationship in the ocean.

Quantifiable OM size–composition relationships might also represent a new way to examine DOM/POM transformation mechanisms. For example, recent work has shown that the spontaneous formation of self-assembled microgels (SAG) and transparent exopolymer particles (TEP; Chin et al. 1998; P. Verdugo unpubl.) acts to "bridge" OM exchange between DOM and POM. However, since assembly likely involves C-rich molecules, the formation macropolymers derived from DOM should result in OM with very high C : N ratios (e.g., TEP C : N $\geq$ 20; Engel and Passow 2001; Mari et al. 2001). If quantitatively significant, the production of SAG and TEP should also result in discontinuities in an OM size–composition trend. Significant marine gel formation processes are therefore inconsistent with the size–composition trends we observe here; however, it is possible that they may be important in oligotrophic environments. Coupled with knowledge of particle aggregate size, OM size–composition relationships might prove useful for investigating the role of DOM/POM transformation mechanisms in different ocean regions.

Finally, the robust correlation between OM size and C : N ratio is a dramatic example of the effect of relative OM size on bulk composition and may have important implications for understanding the transport and fate of coastal OM. Our observations also suggest that similar size–composition relationships may be present in other ocean regions. If a ubiquitous OM size–elemental composition relationship exists, this would imply that physical transport (largely based on size), elemental ratio, and lability can be explicitly predicted—and may represent a powerful new tool for modeling ocean carbon and nitrogen fluxes in biogeochemical cycles.

Acknowledgments

Bryn Phillips, Katie Siegler, and the staff of the Granite Canyon Marine Pollution Studies Laboratory (GCMPSL) provided facilities capable of biweekly and large-volume seawater suspended particulate and dissolved organic matter isolations. Kristine Okimura, Jennifer Lehman, Leslie Roland, Kona Walker, Gemma Vila Reixach, and Maria Calleja (University of California, Santa Cruz) helped perform fieldwork and sample collection. Dyke Andreasen of the University of California, Santa Cruz Stable Isotope Laboratory aided with stable isotopic analysis. Rob Franks of the University of California, Santa Cruz Marine Analytical Laboratory and Melissa Foley and Misty Blakely (University of California, Santa Cruz) aided in nutrient analysis. We also thank two anonymous reviewers and R. Kudela, G. Rau, T. Guilderson, A. Pearson, D. Hansell, A. Knapp, and D. Bronk for their comments, which greatly improved this manuscript. This work was funded by the Friends of Long Marine Lab Student Research Awards (to B.D.W.), the University of California, Santa Cruz–Science, Technology, Engineering, Policy and Society, Institute for Innovation in Environmental Research (to B.D.W.), the University of California, Santa Cruz Center for the Dynamics and Evolution of the Land-Sea Interface (to B.D.W.), the Earl H. Myers and Ethel M. Myers Oceanographic and Marine Biology Trust (to B.D.W.), and the University of California, Santa Cruz Institute of Geophysics and Planetary Physics (to B.D.W. and M.D.M.).

References

Altabet, M. A. 1988. Variations in nitrogen isotopic composition between sinking and suspended particles: Implications for nitrogen cycling and particle transformation in the open ocean. Deep-Sea Res. **35:** 535–545.

———, C. Pilskaln, R. Thunell, C. Pride, D. Sigman, F. Chavez, and R. Francois. 1999. The nitrogen isotope biogeochemistry of sinking particles from the margin of the Eastern North Pacific. Deep-Sea Res. I **46:** 655–679, doi:10.1016/S0967-0637(98)00084-3

Alvarez-Salgado, X. A., M. D. Doval, A. V. Borges, I. Joint, M. Frankignoulle, E. M. S. Woodward, and F. G. Figueiras. 2001*a*. Off-shelf fluxes of labile materials by an upwelling filament in the NW Iberian Upwelling System. Prog. Oceanogr. **51:** 321–337, doi:10.1016/S0079-6611(01)00073-8

———, J. Gago, B. M. Miguez, and F. F. Perez. 2001*b*. Net ecosystem production of dissolved organic carbon in a coastal upwelling system: The Ria de Vigo, Iberian margin of the North Atlantic. Limnol. Oceanogr. **46:** 135–147, doi:10.4319/lo.2001.46.1.0135

Amon, R. M. W., and R. Benner. 1994. Rapid cycling of high molecular weight dissolved organic matter in the ocean. Nature **369:** 549–552, doi:10.1038/369549a0

———, and ———. 1996. Bacterial utilization of different size classes of dissolved organic matter. Limnol. Oceanogr. **41:** 41–51, doi:10.4319/lo.1996.41.1.0041

Bac, M. G., K. R. Buck, F. P. Chavez, and S. C. Brassell. 2003. Seasonal variation in alkenones, bulk suspended POM, plankton and temperature in Monterey Bay, California: Implications for carbon cycling and climate assessment. Org. Geochem. **34:** 837–855, doi:10.1016/S0146-6380(02)00248-6

Barth, J., T. Cowles, P. Kosro, R. Shearman, A. Huyer, and R. L. Smith. 2002. Injection of carbon from the shelf to offshore beneath the euphotic zone in the California Current. J. Geophys. Res. **107:** 3057, doi:10.1029/2001JC000956

Bauer, J. E., and E. R. M. Druffel. 1998. Ocean margins as a significant source of organic matter to the deep open ocean. Nature **392:** 482–485, doi:10.1038/33122

Benner, R., B. Biddanda, B. Black, and M. McCarthy. 1997. Abundance, size distribution, and stable carbon and nitrogen isotopic compositions of marine organic matter isolated by tangential-flow ultrafiltration. Mar. Chem. **57:** 243–263, doi:10.1016/S0304-4203(97)00013-3

———, J. D. Pakulski, M. McCarthy, J. I. Hedges, and P. G. Hatcher. 1992. Bulk chemical characteristics of dissolved organic matter in the ocean. Science **255:** 1561–1564, doi:10.1126/science.255.5051.1561

Breaker, L. C. 2005. What's happening in Monterey Bay on seasonal to interdecadal time scales. Cont. Shelf Res. **25:** 1159–1193, doi:10.1016/j.csr.2005.01.003

Bronk, D. A. 2002. Dynamics of DON, p. 153–247. *In* D. A. Hansell and C. A. Carlson [eds.], Biogeochemistry of marine dissolved organic matter. Academic Press.

———, M. W. Lomas, P. M. Glibert, K. J. Schukert, and M. P. Sanderson. 2000. Total dissolved nitrogen analysis: Comparisons between the persulfate, UV and high temperature oxidation methods. Mar. Chem. **69:** 163–178, doi:10.1016/S0304-4203(99)00103-6

———, and B. B. Ward. 1999. Gross and net nitrogen uptake and DON release in the euphotic zone of Monterey Bay, California. Limnol. Oceanogr. **44:** 573–585, doi:10.4319/lo.1999.44.3.0573

Bruland, K. W., E. L. Rue, and G. J. Smith. 2001. Iron and macronutrients in California coastal upwelling regimes: Implications for diatom blooms. Limnol. Oceanogr. **46:** 1661–1674, doi:10.4319/lo.2001.46.7.1661

Carlson, C. A. 2002. Production and removal processes, p. 91–151. *In* D. A. Hansell and C. A. Carlson [eds.], Biogeochemistry of marine dissolved organic matter. Academic Press.

———, and others. 2010. Dissolved organic carbon export and subsequent remineralization in the mesopelagic and bathypelagic realms of the North Atlantic basin. Deep-Sea Res. II **57:** 1433–1445, doi:10.1016/j.dsr2.2010.02.013

Cermeno, P., E. Maranon, J. Rodriguez, and E. Fernandez. 2005. Large-sized phytoplankton sustain higher carbon-specific photosynthesis than smaller cells in a coastal eutrophic ecosystem. Mar. Ecol. Prog. Ser. **297:** 51–60, doi:10.3354/meps297051

Chavez, F. P., and J. R. Toggweiler. 1995. Physical estimates of global new production: The upwelling contribution. John Wiley.

Chesselet, R., M. Fontugne, P. Buatmenard, U. Ezat, and C. E. Lambert. 1981. The origin of particulate organic carbon in the marine atmosphere as indicated by its stable carbon isotopic composition. Geophys. Res. Lett. **8:** 345–348, doi:10.1029/GL008i004p00345

Chin, W. C., M. V. Orellana, and P. Verdugo. 1998. Spontaneous assembly of marine dissolved organic matter into polymer gels. Nature **391:** 568–572, doi:10.1038/35345

Close, H. G., R. Bovee, and A. Pearson. 2011. Inverse carbon isotope patterns of lipids and kerogen record heterogeneous primary biomass. Geobiology **9:** 250–265, doi:10.1111/j.1472-4669.2011.00273.x

Cowie, G. L., and J. I. Hedges. 1994. Biochemical indicators fo diagenetic alteration in natural organic matter mixtures. Nature **369:** 304–307, doi:10.1038/369304a0

Druffel, E. R. M., J. E. Bauer, P. M. Williams, S. Griffin, and D. Wolgast. 1996. Seasonal variability of particulate organic radiocarbon in the northeast Pacific ocean. J. Geophys. Res. **101:** 20543–20552, doi:10.1029/96JC01850

———, P. M. Williams, J. E. Bauer, and J. R. Ertel. 1992. Cycling of dissolved and particulate organic matter in the open ocean. J. Geophys. Res. **97:** 15639–15659, doi:10.1029/92JC01511

Engel, A., and U. Passow. 2001. Carbon and nitrogen content of transparent exopolymer particles (TEP) in relation to their Alcian Blue adsorption. Mar. Ecol. Prog. Ser. **219:** 1–10, doi:10.3354/meps219001

Fawcett, S. E., M. W. Lomas, J. R. Casey, B. B. Ward, and D. M. Sigman. 2011. Assimilation of upwelled nitrate by small eukaryotes in the Sargasso Sea. Nat. Geosci. **4:** 717–722, doi:10.1038/ngeo1265

Flament, P. 2002. A state variable for characterizing water masses and their diffusive stability: Spiciness. Prog. Oceanogr. **54:** 493–501, doi:10.1016/S0079-6611(02)00065-4

Fogg, G. E. 1983. The ecological significance of extracellular products of phytoplankton photosynthesis. Bot. Mar. **26:** 3–14, doi:10.1515/botm.1983.26.1.3

Foley, M. M., and P. L. Koch. 2010. Correlation between allochthonous subsidy input and isotopic variability in the giant kelp Macrocystis pyrifera in central California, USA. Mar. Ecol. Prog. Ser. **409:** 41–50, doi:10.3354/meps08600

Goldberg, S. J., C. A. Carlson, D. A. Hansell, N. B. Nelson, and D. A. Siegel. 2009. Temporal dynamics of dissolved combined neutral sugars and the quality of dissolved organic matter in the Northwestern Sargasso Sea. Deep-Sea Res. I **56:** 672–685, doi:10.1016/j.dsr.2008.12.013

Hales, B. T., M. Takahashi, and L. Bandstra. 2005. Atmospheric CO2 uptake by a coastal upwelling system. Glob. Biogeochem. Cycles **19:** GB1009, doi:10.1029/2004GB002295

Hansell, D. A. 2005. Dissolved organic carbon reference material program. EOS, Trans. Am. Geophys. Union **86:** 318–319, doi:10.1029/2005EO350003

———, and C. A. Carlson. 2001. Biogeochemistry of total organic carbon and nitrogen in the Sargasso Sea: Control by convective overturn. Deep-Sea Res. II **48:** 1649–1667, doi:10.1016/S0967-0645(00)00153-3

———, and T. Y. Waterhouse. 1997. Controls on the distributions of organic carbon and nitrogen in the eastern Pacific Ocean. Deep-Sea Res. I **44:** 843–857, doi:10.1016/S0967-0637(96)00128-8

———, P. M. Williams, and B. B. Ward. 1993. Measurements of DOC and DON in the Southern California Bight using oxidation by high-temperature combustion. Deep-Sea Res. I **40:** 219–234, doi:10.1016/0967-0637(93)90001-J

Hernes, P. J., and R. Benner. 2002. Transport and diagenesis of dissolved and particulate terrigenous organic matter in the North Pacific Ocean. Deep-Sea Res. I **49:** 2119–2132, doi:10.1016/S0967-0637(02)00128-0

Hill, J. K., and P. A. Wheeler. 2002. Organic carbon and nitrogen in the northern California current system: Comparison of offshore, river plume, and coastally upwelled waters. Prog. Oceanogr. **53:** 369–387, doi:10.1016/S0079-6611(02)00037-X

Hopkinson, C. S., and J. J. Vallino. 2005. Efficient export of carbon to the deep ocean through dissolved organic matter. Nature **433:** 142–145, doi:10.1038/nature03191

Hutchins, D. A., and K. W. Bruland. 1998. Iron-limited diatom growth and Si : N uptake ratios in a coastal upwelling regime. Nature **393:** 561–564, doi:10.1038/31203

Kaiser, K., and R. Benner. 2008. Major bacterial contribution to the ocean reservoir of detrital organic carbon and nitrogen. Limnol. Oceanogr. **53:** 99–112, doi:10.4319/lo.2008.53.1.0099

———, and ———. 2009. Biochemical composition and size distribution of organic matter at the Pacific and Atlantic time-series stations. Mar. Chem. **113:** 63–77, doi:10.1016/j.marchem.2008.12.004

Knapp, A. N., D. Sigman, F. Lipschultz, A. B. Kustka, and D. G. Capone. 2011. Interbasin isotopic correspondence between upper-ocean bulk DON and subsurface nitrate and its implications for marine nitrogen cycling. Glob. Biogeochem. Cycles **25:** 1–14, doi:10.1029/2010GB003878

Knepel, K., and K. Bogren. 2002. Determination of orthophosphate by flow injection analysis. QuikChem method 31-115-01-H. *In* Methods manual. Lachat Instruments.

Libby, P. S., and P. A. Wheeler. 1997. Particulate and dissolved organic nitrogen in the central and eastern equatorial Pacific. Deep-Sea Res. I **44:** 345–361, doi:10.1016/S0967-0637(96)00089-1

Loh, A. N., and J. E. Bauer. 2000. Distribution, partitioning and fluxes of dissolved and particulate organic C, N and P in the eastern North Pacific and Southern Oceans. Deep-Sea Res. I **47:** 2287–2316, doi:10.1016/S0967-0637(00)00027-3

———, ———, and E. R. M. Druffel. 2004. Variable ageing and storage of dissolved organic components in the open ocean. Nature **430:** 877–881, doi:10.1038/nature02780

Lomas, M. W., and P. M. Glibert. 1999. Temperature regulation of nitrate uptake: A novel hypothesis about nitrate uptake and reduction in cool-water diatoms. Limnol. Oceanogr. **44:** 556–572, doi:10.4319/lo.1999.44.3.0556

Mari, X., S. Beauvais, R. Lemee, and M. L. Pedrotti. 2001. Non-Redfield C : N ratio of transparent exopolymeric particles in the northwestern Mediterranean Sea. Limnol. Oceanogr. **46:** 1831–1836, doi:10.4319/lo.2001.46.7.1831

McCarthy, M. D., R. Benner, C. Lee, and M. L. Fogel. 2007. Amino acid nitrogen isotopic fractionation patterns as indicators of heterotrophy in plankton, particulate, and dissolved organic matter. Geochim. Cosmochim. Acta **71:** 4727–4744, doi:10.1016/j.gca.2007.06.061

———, ———, ———, J. I. Hedges, and M. L. Fogel. 2004. Amino acid carbon isotopic fractionation patterns in oceanic dissolved organic matter: An unaltered photoautotrophic source for dissolved organic nitrogen in the ocean? Mar. Chem. **92:** 123–134, doi:10.1016/j.marchem.2004.06.021

———, J. I. Hedges, and R. Benner. 1998. Major bacterial contribution to marine dissolved organic nitrogen. Science **281:** 231–234, doi:10.1126/science.281.5374.231

Meador, T. B., L. I. Aluwihare, and C. Mahaffey. 2007. Isotopic heterogeneity and cycling of organic nitrogen in the oligotrophic ocean. Limnol. Oceanogr. **52:** 934–947, doi:10.4319/lo.2007.52.3.0934

Muller-Karger, F. E., R. Varela, R. Thunell, R. Luerssen, C. M. Hu, and J. J. Walsh. 2005. The importance of continental margins in the global carbon cycle. Geophys. Res. Lett. **32:** L01602, doi:10.1029/2004GL021346

Munk, W. 1981. Internal waves and small-scale processes, p. 264–291. *In* B. A. Warren and W. C. [eds.], Evolution of physical oceanography. MIT Press.

Nieto-Cid, M., X. A. Alvarez-Salgado, S. Brea, and F. F. Perez. 2004. Cycling of dissolved and particulate carbohydrates in a coastal upwelling system (NW Iberian Peninsula). Mar. Ecol. Prog. Ser. **283:** 39–54, doi:10.3354/meps283039

Pennington, J. T., and F. P. Chavez. 2000. Seasonal fluctuations of temperature, salinity, nitrate, chlorophyll and primary production at station H3/M1 over 1989–1996 in Monterey Bay, California. Deep-Sea Res. II **47:** 947–973, doi:10.1016/S0967-0645(99)00132-0

Pierce, S. D., R. L. Smith, P. M. Kosro, J. A. Barth, and C. D. Wilson. 2000. Continuity of the poleward undercurrent along the eastern boundary of the mid-latitude north Pacific. Deep-Sea Res. II **47:** 811–829, doi:10.1016/S0967-0645(99)00128-9

Raimbault, P., and others. 1999. Carbon and nitrogen uptake and export in the equatorial Pacific at 150 degrees W: Evidence of an efficient regenerated production cycle. J. Geophys. Res. Oceans **104:** 3341–3356, doi:10.1029/1998JC900004

Rau, G. H., J. L. Teyssie, F. Rassoulzadegan, and S. W. Fowler. 1990. C-13/C-12 and N-15/N-14 variations among size-fractionated marine particles: Implications for their origin and trophic relationships. Mar. Ecol. Prog. Ser. **59:** 33–38, doi:10.3354/meps059033

Repeta, D. J., and L. I. Aluwihare. 2006. Radiocarbon analysis of neutral sugars in high-molecular-weight dissolved organic carbon: Implications for organic carbon cycling. Limnol. Oceanogr. **51:** 1045–1053, doi:10.4319/lo.2006.51.2.1045

Roland, L. A., M. D. McCarthy, T. D. Peterson, and B. D. Walker. 2009. A large-volume micro-filtration system for isolating suspended particulate organic matter: Fabrication and assessment vs. GF/F filters in central N. Pacific. Limnol. Oceanogr.: Methods **7:** 64–80, doi:10.4319/lom.2009.7.64

Sannigrahi, P., E. D. Ingall, and R. Benner. 2005. Cycling of dissolved and particulate organic matter at station Aloha: Insights from C-13 NMR spectroscopy coupled with elemental, isotopic and molecular analyses. Deep-Sea Res. I **52:** 1429–1444, doi:10.1016/j.dsr.2005.04.001

Sharp, J. H., and others. 2002. A preliminary methods comparison for measurement of dissolved organic nitrogen in seawater. Mar. Chem. **78:** 171–184, doi:10.1016/S0304-4203(02)00020-8

Shkedy, Y., D. Fernandez, C. Teague, J. Vesecky, and J. Roughgarden. 1995. Detecting upwelling along the central coast of California during an El Nino year using HF-Radar. Cont. Shelf Res. **15:** 803–814, doi:10.1016/0278-4343(94)00042-L

Skogsberg, T. 1936. Hydrography of Monterey Bay, California. Thermal conditions, 1929–1933. Trans. Am. Phil. Soc. **29:** 1–152, doi:10.2307/1005510

———, and A. Phelps. 1946. Hydrography of Monterey Bay, California. Thermal conditions, part II, 1934–1937. Proc. Am. Phil. Soc. **90:** 350–386.

Smayda, T. J. 1997. Harmful algal blooms: Their ecophysiology and general relevance to phytoplankton blooms in the sea. Limnol. Oceanogr. **42:** 1137–1153, doi:10.4319/lo.1997.42.5_part_2.1137

Smith, P., and K. Bogren. 2001*a*. Determination of nitrate and/or nitrite in brackish or seawater by flow injection analysis colorimetry. QuikChem method 31-107-04-1-C. *In* Methods manual. Lachat Instruments.

———, and ———. 2001*b*. Determination of silicate in brackish or seawater by flow injection analysis colorimeter. QuikChem method 31-114-27-1-C. *In* Methods manual. Lachat Instruments.

UNESCO. 1981. Background papers and supporting data on the Practical Salinity Scale, 1978. UNESCO Tech. Pap. Mar. Sci., No. 37.

Walker, B. D., S. R. Beaupre, T. P. Guilderson, E. R. M. Druffel, and M. D. McCarthy. 2011. Large-volume ultrafiltration for the study of radiocarbon signatures and size vs. age relationships in marine dissolved organic matter. Geochim. Cosmochim. Acta **75:** 5187–5202, doi:10.1016/j.gca.2011.06.015

WARD, B. B., AND D. A. BRONK. 2001. Net nitrogen uptake and DON release in surface waters: Importance of trophic interactions implied from size fractionation experiments. Mar. Ecol. Prog. Ser. **219:** 11–24, doi:10.3354/meps219011

WETZ, M. S., AND P. A. WHEELER. 2003. Production and partitioning of organic matter during simulated phytoplankton blooms. Limnol. Oceanogr. **48:** 1808–1817, doi:10.4319/lo.2003.48.5.1808

———, AND ———. 2007. Release of dissolved organic matter by coastal diatoms. Limnol. Oceanogr. **52:** 798–807, doi:10.4319/lo.2007.52.2.0798

WILLIAMS, P. J. L. 1995. Evidence for the seasonal accumulation of carbon-rich dissolved organic material, its scale in comparison with changes in particulate material and the consequential effect on net C/N assimilation ratios. Mar. Chem. **51:** 17–29, doi:10.1016/0304-4203(95)00046-T

Associate editor: Robert R. Bidigare

Received: 22 December 2011
Accepted: 21 July 2012
Amended: 02 August 2012